Bulletin of the Geological Survey of Japan, vol. 43 (4), p. 257-284, 1992

Hydrothermal manganese oxide deposits from the Izu-Ogasawara(Bonin)-Mariana Arc and adjacent areas

Akira USUI* and Akira NISHIMURA*

USUI, Akira and NISHIMURA, Akira (1992) Hydrothermal manganese oxide deposits from the Izu-Ogasawara (Bonin) -Mariana Arc and adjacent areas. *Bull. Geol. Surv. Japan*, vol. 43 (4), p. 257-284, 7 fig., 3 tab., 3pl.

Abstract : Modern and fossil hydrothermal manganese deposits were discovered from a number of locations in active and inactive submarine volcanoes (Bonin, Mariana, and Kyushu-Palau arcs) and a backarc rift (Sumisu Rift) during the Hakurei-Maru cruises in 1984 to 1989. The mineralogical and chemical composition and microstructure of the deposits are typically different from manganese nodules and crusts of hydrogenetic or diagenatic origin. Hardpans, veinlets, sheets and irregular mass of the hydrothermal manganese deposits often cover a large area of sea bed, suggesting possible high-temperature hydrothermal sulfide deposits in their vicinity. On the other hand, the manganese minerals sometimes occur as substrate of younger hydrogenetic crusts and as nucleus of hydrogenetic nodules, which can be geological records of low-temperature hydrothermal activity on the past island arcs.

1. Introduction

Marine ferromanganese deposits are in principal composed of hydrogenetic, hydrothermal and diagenetic manganese minerals, and occur as nodules, crusts, aggregates, stains etc. The hydrothermal manganese deposits are different from deep-sea nodules or crusts in their chemistry, mineralogy and origin. Hydrothermal manganese deposits were first found in active mid-oceanic spreading centers, somewhat apart from high-temperature hydrothermal sites, in the East Pacific Rise and the Mid-Atlantic Ridge (Scott *et al.*, 1976a ; Corliss *et al.*, 1978). Cronan *et al.*, (1982) reported the first occurrence of island-arc submarine hydrothermal manganese deposits from the Tonga-Kermadec Arc, the South Pacific. However, little has been known on the nature and distribution of these deposits in other island-arcs. This paper focuses on description of hydrothermal manganese oxide deposits of the Izu-Ogasawara Arc and Kyushu-Palau Ridge, based on results from our cruises in the West Pacific.

*Marine Geology Department

The geological setting of the Izu-Ogasawara arc, where spreading is assumed in the Quaternary age (Karig and Moore, 1975 ; Taylor *et al.*, 1984 ; Honza and Tamaki, 1985), implies an on-going hydrothermal activity in its back-arc rifts. During the cruises with R/V Hakurei-Maru from 1984 to 1989 as part of the 6-year program "Hydrothermal Activity in the Izu-Ogasawara Arc" , a number of hydrothermal and hydrogenetic manganese deposits were collected mostly around topographic highs both in active and inactive areas (Fig. 1).

2. Ship-board survey and laboratory technique

Two cruises of R/V Hakurei-Maru were conducted each year by the Geological Survey of Japan (GSJ) from 1984 through 1988 and one in 1989 in the areas including Izu-Ogasawara-Mariana Arc, Ogasawara Plateau, and Kyushu-Palau Ridge in the West Pacific. Bathymetric and seis-

Keywords : manganese minerals, hydrothermal, submarine volcano, todorokite, buserite, Izu-Ogasawara, Kyushu-Palau, Mariana

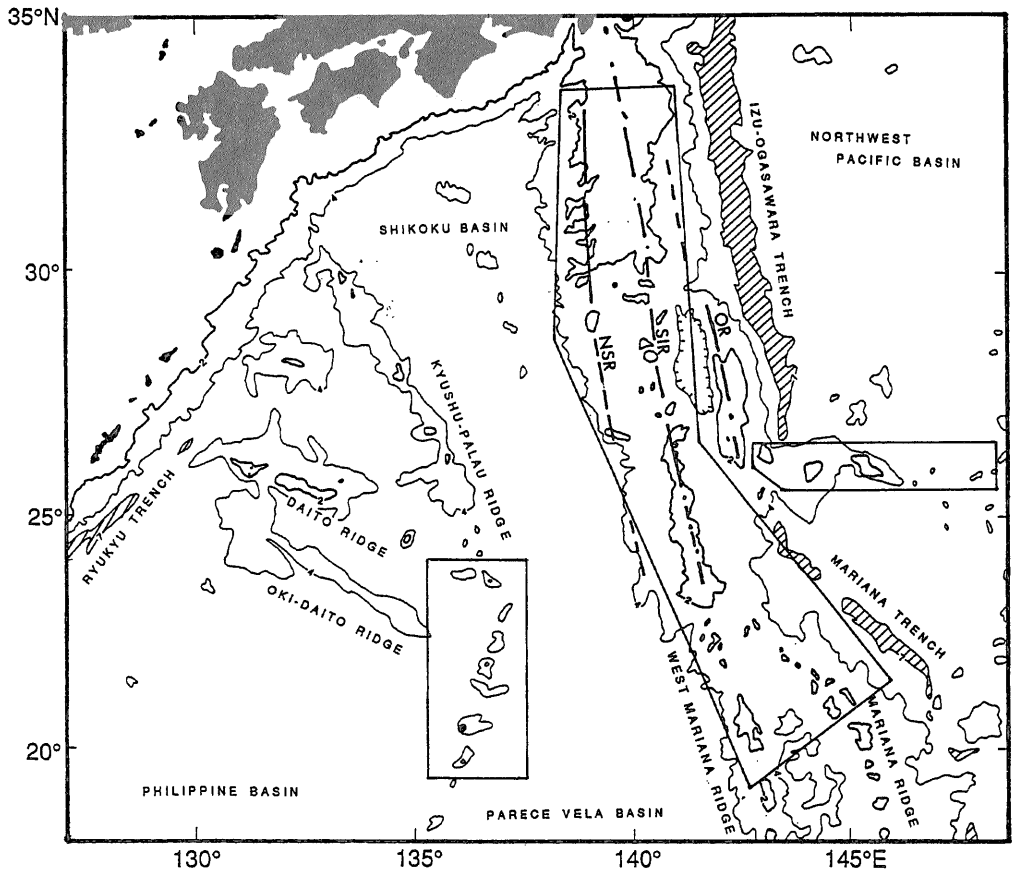

Fig. 1 Survey area of the GSJ program "Hydrothermal activity in the Izu-Ogasawara Arc (1984-1989)". Most sampling and geophysical survey were focussed on the three enclosed boxes in the map. NSR : Nishi-Shichito Ridge, SIR : Shichito-Iwojima Ridge, OR : Ogasawara Ridge. SIR and Mariana Ridge are the only active ridges in the survey area.

mic surveys were carried out with air gun, 3.5 kHz SBP, 12 kHz PDR, followed by bottom sampling, camera towing, side-looking sonar mapping, TV observation, water sampling, heat flow measurement, and ocean bottom seismometer survey. Bottom materials were collected by dredge, corers and grabs. Some hydrothermal manganese deposits were observed by manned deep submersibles ALVIN (Woods Hole Oceanographic Institution) at the Sumisu Rift and SHINKAI 2000 (Japan Marine Science and Technology Center) at the Kaikata Seamount.

Manganese oxide samples were soaked in sea water and stored in a refrigerator immediately after recovery to prevent drying and mineralogical transformation (Usui *et al.*, 1989). Subsamples taken from each hand specimen were subjected to X-ray powder diffraction (XRD) analysis in wet and air-dried conditions to ascertain structural stability during dehydration. Dried samples at 110℃ for 3 hours were analyzed for their chemical composition by atomic absorption spectroscopy according to the GSJ standard procedures (Terashima, 1978). Analytical uncertainty was checked against USGS rock standards, Nod-P-1 and Nod-A-1 (Franagan and Gottfried, 1980). Microstructure was observed with scanning electron microscope (SEM) and reflecting microscope. Several subsamples were selected for U-Th age determination.

3. Survey area and regional setting

The survey areas of the eleven cruises cover the Izu-Ogasawara-Mariana arc and Kyushu-Palau Ridge between 19°N and 34°N (Fig. 1). Rock sampling was performed at more than 330 stations mainly around topographic highs. More then 100 bottom samples were collected at the Kaikata Seamount, a member of active Izu-Ogasawara volcanic chain for the purpose of mapping hydrothermal manganese deposits on the sea floor (Figs. 2 and 3).

The Izu-Ogasawara arc, trending north to south, includes three major ridges. The Shichito-Iwojima Ridge consists of active submarine volcanoes and volcanic islands, forming the volcanic front. Two remnant inactive ridges on the Tertiary basements, (Nishi-Shichito Ridge to the west and Ogasawara Ridge to the east) run nearly parallel to the Shichito-Iwojima ridge. Recent rifting of the sea floor and hydrothermal activity (Urabe and Kusakabe, 1990) are assumed at the back-arc depressions between the Shichito-Iwojima Ridge and the Nishi-Shichito Ridge (Tamaki, 1985 ; Yamazaki, 1988 ; Murakami, 1988 ; Brown and Taylor, 1988). In the Sumisu Rift, one of these back-arc depressions, silica and barite chimneys were discovered with ALVIN.

The Kyushu-Palau Ridge is believed to be formed at an ancient island-arc system prior to the opening of the Parece Vela Basin from 17 Ma to 25 Ma (Seno and Maruyama, 1984). The oldest K-Ar age of dredged rocks from the ridge is 48.5 Ma (Mizuno *et al.*, 1977). Ogasawara Ridge is considered to be a Paleogene island arc formed by forearc rifting during the Oligocene time (Leg 126 Shipboard Party, 1989).

4. Description of hydrothermal manganese and iron deposits

The first occurrence of submarine hydrothermal manganese deposits was described around the mid-oceanic ridge spreading centers (Scott *et al.*, 1976a ; Corliss *et al.*, 1978). These deposits occur in various forms like stratified dense sheets, crusts, veinlets and various aggregates at seamounts, fracture zones, mounds etc. (Moore and Vogt, 1976 ; Lonsdale *et al.*, 1980). It is estimated that the growth rate of a hydrothermal crust is more than two orders of magnitude greater than those of deep-sea nodules and crusts (Scott *et al.*, 1976b). Cronan *et al.* (1982) reported similar hydrothermal manganese deposits in Tonga-Kermadec arc in the South Pacific. Hein *et al.* (1987) reported extensive distribution of these deposits in the active Mariana volcanic chain.

The hydrothermal manganese deposits from the Izu-Ogasawara Arc (Usui *et al.*, 1986) consist typically dense, gray and submetallic layers or cusps, similar in appearance and conposition to those from the mid-oceanic ridge spreading centers (Plate I). The dense gray layers of hydrothermal manganese oxide from the Kaikata Seamount range in thickness from a few to 30 mm. These layers are overlain by volcanic sand layer cemented by manganate matrix (Plate I-A). This sequence shows that hydrothermal solutions have supplied manganese from substrates which precipitate new surfaces just beneath the uppermost sand layers. The similar deposits from the Sumisu Rift show more than 4 cm thick dense submetallic layers, which are scarcely covered by hydrogenetic ferromanganese oxide layers.

Other hydrothermal manganese deposits from the Nishi-Shichito Ridge, the Ogasawara Ridge, and Kyushu-Palau Ridge are always covered by younger hydrogenetic ferromanganese layers(Plate I-B/lower and I-C). Hydrothermal manganese deposits usually serve as nuclei of spheroidal nodules or as substrates of ferromanganese crusts, suggesting a ceased hydrothermal activity in the areas.

5. Chemistry

The chemical composition of the studied manganese deposit is clearly different from hydrogenetic or diagenetic deposits. The most remarkable difference is their very high Mn/Fe ratio (much greater than 10) and very low concentration of transition metal elements, such as Cu, Ni, Zn, Co, and Pb. Though mineralogy of hydrothermal manganate is still controversial, they always consist of 10 Å and/or 7 Å manganates after air drying at a room temperature. The crystal has elongated blade-like habit up to one millimeter in

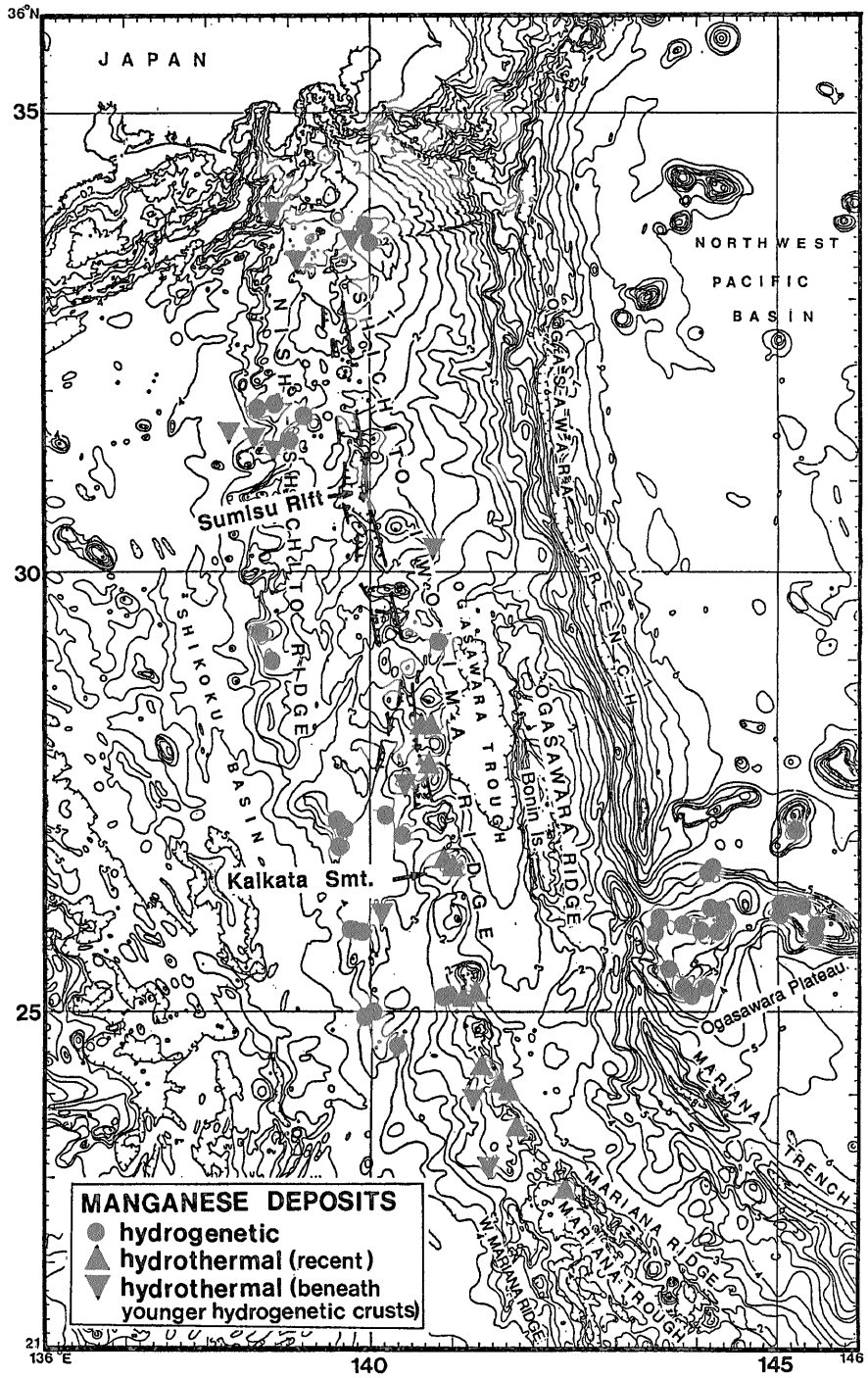

Fig. 2 Distribution of hydrothermal and hydrogenetic manganese deposits in the Izu-Ogasawara Arc. The recent hydrothermal deposits are dominant in seamounts in the volcanic front (SIR). Fossil hydrothermal deposits are distributed in the two remnant ridges of Tertiary (NSR, OR). A chain of back-arc depressions runs along the front.

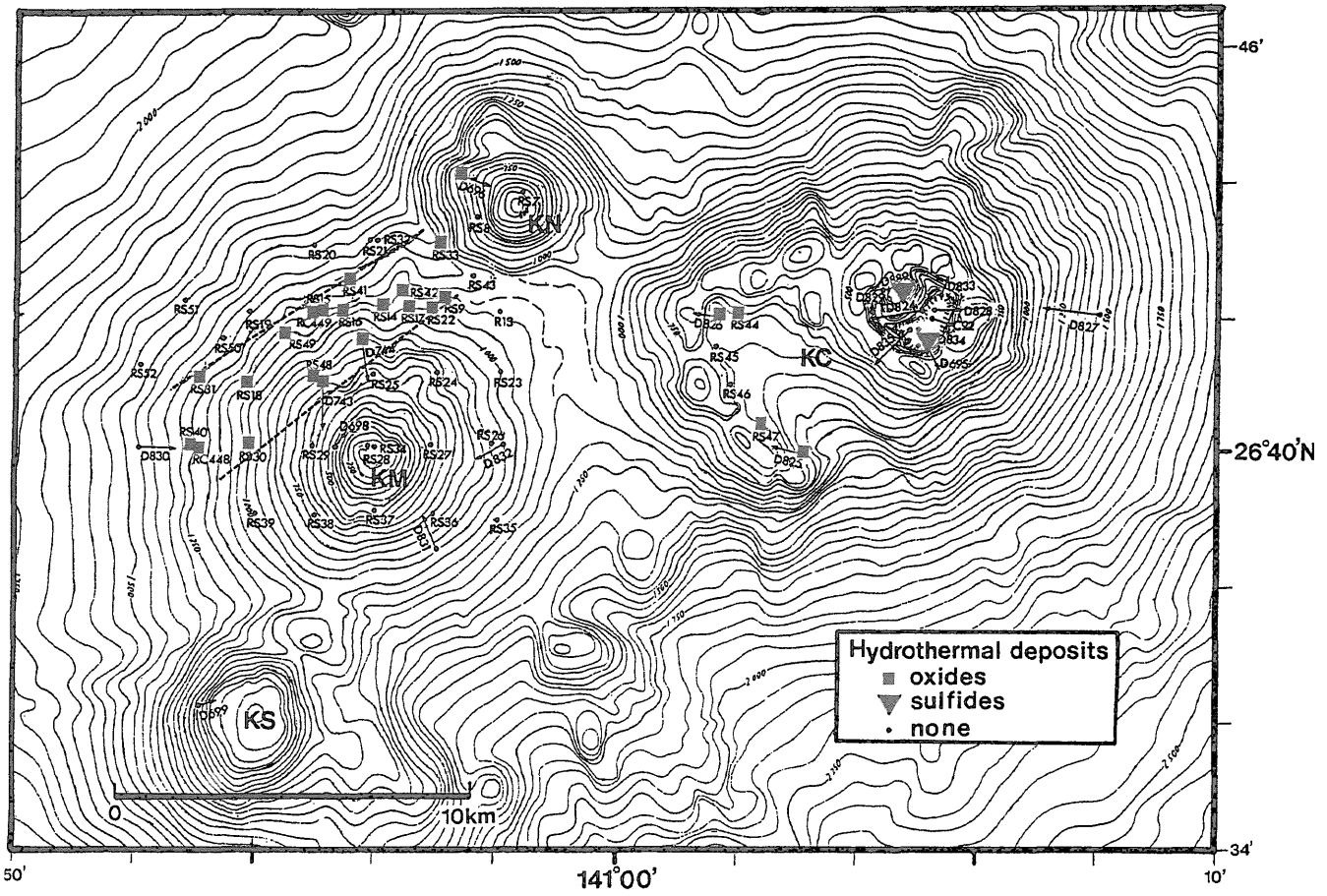

Fig. 3 Distribution of hydrothermal deposits in the Kaikata Seamount. A solid square denotes occurrence of thick submetallic layer of hydrothermal manganese oxide deposits and a triangle sulfide mineralization. The belt in the northwest slope of the KM peak is the field of distribution of hydrothermal manganese deposits.

long axis. Usui *et al.* (1989) proposed that these hydrothemal manganates are varieties of todorokite series which differ from the phyllomanganate of diagenetic buserite series from deep-sea manganese nodules.

The detritus-free nature of these hydrothermal manganate deposits is recognized in their chemical composition. The samples taken from recent submarine volcanoes in the Izu-Ogasawara Arc and adjacent inactive ridges are similarly of very low concentrations in silica, alumina and minor heavy metal elements, like Fe, Cu, Ni, Co, Zn, and Pb (Table 1 and Fig. 4). The Mn/Fe ratio ranges from 10 to 4000 and Fe concentration is usually less than 1 %. Concentrations of Cu, Ni, Co, Zn, and Pb range from less than 1 ppm to 1000 ppm,

Table 1 Chemical and mineral composition of hydrothermal manganates and iron deposits from Izu-Ogasawara Arc.

PROVINCES	SAMPLE NO.	MINERALOGY (air-dried at R.T.)				CHEMISTRY (110°C-dried base)								DESCRIPTION	AREA
		10Å	7Å	X(10/7)	others	Mn wt.%	Fe wt.%	Mn/Fe	Cu ppm	Ni ppm	Zn ppm	Co ppm	Pb ppm		
volcanic front	D792-1#2	41	2	21	-	46.40	1.59	29	414	585	429	146	93	small cusps	seamount
	D792-1#1	29	13	2.2	-	41.45	0.41	101	681	362	281	10	22	dense layer	seamount
	D791-6	8	42	0.2	c	43.88	0.55	80	426	225	262	108	13	small cusps	seamount
	D817-7	82	14	5.9	-	43.93	0.15	293	466	50	53	57	10	soft clay	Fukutoku smt.
	D817-6	38	7	5.4	-	45.08	0.38	119	133	260	167	19	2	small cusps	Fukutoku smt.
	D817-25	15d	15d	1	-	40.01	0.22	182	954	40	94	18	5	dense layer	Fukutoku smt.
	D821-2	29	13	2.2	-	39.28	3.67	11	222	899	345	209	27	veinlet	Kita-Iwo Jima Is.
	D825-10	37	20	1.9	-	39.73	0.15	265	35	88	101	8	10	dense layer	peak KC, Kaikata smt.
	D826-11	39	37	1.1	-	45.86	0.29	158	22	6	32	10	13	dense layer	peak KC, Kaikata smt.
	RC449#2	164	0	∞	c	45.15	0.51	89	355	45	61	34	14	dense layer	peak KM, Kaikata smt.
	RS9	++				43.00	0.07	614	139	6	14	27	2	dense layer	peak KM, Kaikata smt.
	RS16-2	+	++	+	p	31.10	2.04	15	52	40	52	14	6	dense layer	peak KM, Kaikata smt.
	RS16-3	+	++	+	-	36.80	1.21	30	327	10	38	34	5	dense layer	peak KM, Kaikata smt.
	RS164	++	+	+	-	33.40	2.37	14	1000	53	65	28	6	dense layer	peak KM, Kaikata smt.
	RS18-5#1	131	0	∞	-	41.13	3.18	13	310	1	22	21	1	dense layer	peak KM, Kaikata smt.
	RS18-5#2	190	0	∞	p	37.88	1.35	28	329	25	44	55	14	dense layer	peak KM, Kaikata smt.
	RS304	15	43	0.3	c	40.55	1.01	40	91	177	182	29	23	small cusps	peak KM, Kaikata smt.
	RS31-6	139	0	∞	c	45.28	0.57	79	88	27	48	30	0	fibrous cusps	peak KM, Kaikata smt.
	RS33-3	5	25	0.2	p	28.32	2.89	10	144	168	194	28	16	dense layer	peak KM, Kaikata smt.
	RS40-8#1	0	24	0	-	30.30	2.44	12	161	84	112	35	0	black layer	peak KM, Kaikata smt.
	RS40-8#2	40	18	2.2	p,c	39.34	4.13	10	163	6	30	8	1	dense layer	peak KM, Kaikata smt.
	RS48	77	0	∞	-	46.24	0.23	201	358	5	38	34	18	dense layer	peak KM, Kaikata smt.
backarc(ridge)	D369	+	+	+	-	48.06	0.60	80	373	1120	840	15	10	fragment	Nishi-Shichito ridge
	D634-MN4	11	26	0.4	-	46.70	0.01	4670	91	10	1	36	<10	dense layer	Nishi-Shichito ridge
	D634-nN2	32	23	1.4	c	38.56	0.14	275	169	527	621	52	<10	dense layer	Nishi-Shichito ridge
	D634-MN7	31	14	2.2	q	43.73	0.51	86	637	1403	963	27	54	dense layer	Nishi-Shichito ridge
	D634-MN2A	29	10	2.9	c,q	25.67	0.41	63	280	1179	43	78	<10	porous layer	Nishi-Shichito ridge
	D634-MN3A	58	18	3.2	c,q	28.95	0.43	67	221	452	31	188	<10	porous layer	Nishi-Shichito ridge
	D634-MN3	61	0	∞	-	37.25	0.02	1860	186	64	20	10	<10	dense layer	Nishi-Shichito ridge
	D634-MN6	47	0	∞	-	49.85	0.11	453	169	60	57	109	<10	denseaggreg.	Nishi-Shichitoridge
	D711-1	+	-		p	41.20	1.01	41	65	167	144	77	32	denselayer	WestofKita-Iwols.
	D711-2	+				47.20	0.07	674	20	51	50	19	1	denselayer	WestofKita-Iwols.
	D711-3	+	-	∞	-	45.40	0.15	303	44	156	145	24	1	denselayer	WestofKita-Iwols.
	D802-1	65	0	0	-	50.96	0.23	223	379	1011	754	24	7	nodule nucleus	seamount of back-arc ridge
backarc(rift)	Dv1889-14	65	0		-	47.50	0.07	651	160	391	313	8	na	dense layer	Sumisu Rift
	Dv1889-14	67	0		-	47.90	0.08	622	84	81	151	6	na	dense layer	Sumisu Rift
	Dv1889-14	73	0		-	46.60	0.17	274	53	94	102	14	na	dense layer	Sumisu Rift
	Dv1889-14	75	0	∞	q,p	40.40	1.24	33	60	142	116	8	na	dense layer	Sumisu Rift
forearc(ridge)	D361	+	+	+	-	40.03	0.96	42	825	145	120	60	10	fragment	East of Torishima
	D750-15	+	-	**	pr,cc	34.80	0.76	46	142	302	180	73	56	dense layer	Shin-Kurose
	D798-6	71	2	36	-	50.75	0.06	846	227	482	262	10	21	nodule nucleus	fore-arc high
	D798-9	0	59	0	-	44.94	0.22	204	122	1078	1233	36	32	nodule nucleus	fore-arc high
IRON OXIDES	D817-10	-	-	- amorph		3.62	32.67	0.1	35	7	7	9	10	brown layer	Fukutoku smt.
	RS18	-	-	- amorph		0.69	36.80	0.02	80	200	16	17	41	yellowish clay	peak KM, Kaikata smt.

NOTE/ Mineralogy: X-ray intensity is shown on a relative scale. x(10/7) = ratio of intensity at 10Å and 7Å d-spacings.
++ = strong, + = present, - = not detected, q = quartz, p = plagioclase, c = calcite, pr = pyrolusite, amorph= amorphous.
Chemistry: na = not analyzed.

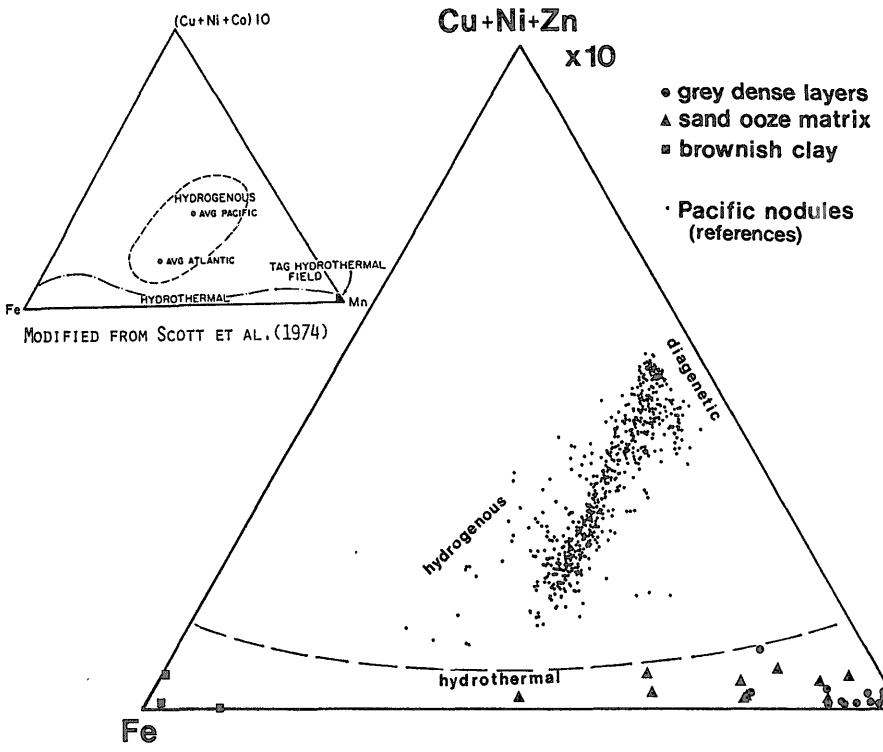

Fig. 4 Ternary diagram showing chemical characters of hydrothermal iron and manganese oxide deposits of this study in comparison with Pacific deep-sea manganese nodules.

with common values lower than 100 ppm. The ranges of variation of these elements are as large as two orders of magnitude. Considerable proportion of these minor elements may be derived from detrital minerals of basic volcanic rocks and glasses. Volcanic rocks contains several tens ppm of Co, Ni, Zn etc. In many cases high concentrations of these elements are associated with high concentration of Fe and/or aluminosilicate mineral in the sample. However, in other cases, high Cu is related to high manganese concentration, suggesting a possibility of lattice-held transition elements in manganate minerals. On the other hand, typical tunnel-structure todorokite accommodate only negligible amount of transition elements, but tend to contain alkali or alkali-earth elements. Variation of transition elements can be attributed to detrital particles included in the deposits, but only a small part may be incorporated in manganate structure.

6. Mineralogy

In recent review articles (Burns and Burns, 1979 ; Arrhenius *et al.*, 1979) ; Giovanoli, 1980 ; Arrhenius and Tsai, 1981 ; Mellin, 1981 ; Burns *et al.*, 1983), mineralogy of marine manganates is discussed in terms of their crystal structure as well as of chemistry. Previous studies suggest that four principal manganese minerals occur in marine hydrothermal, hydrogentic, and diagenetic manganese deposits. These four minerals are often regarded as structural analogues of some terrestrial and synthetic manganese (IV) compounds.

(1) *Todorokite* : A 10 Å manganate with edge-shared MnO_6 octahedra forming a tunnel structure accommodating large cations such as Ba and K (Turner and Buseck, 1981 ; Burns *et al.*, 1983),

(2) *Buserite* : A synthetic 10 Å phyllomanganate in which interlayer $[MnO_6]$ walls are absent but

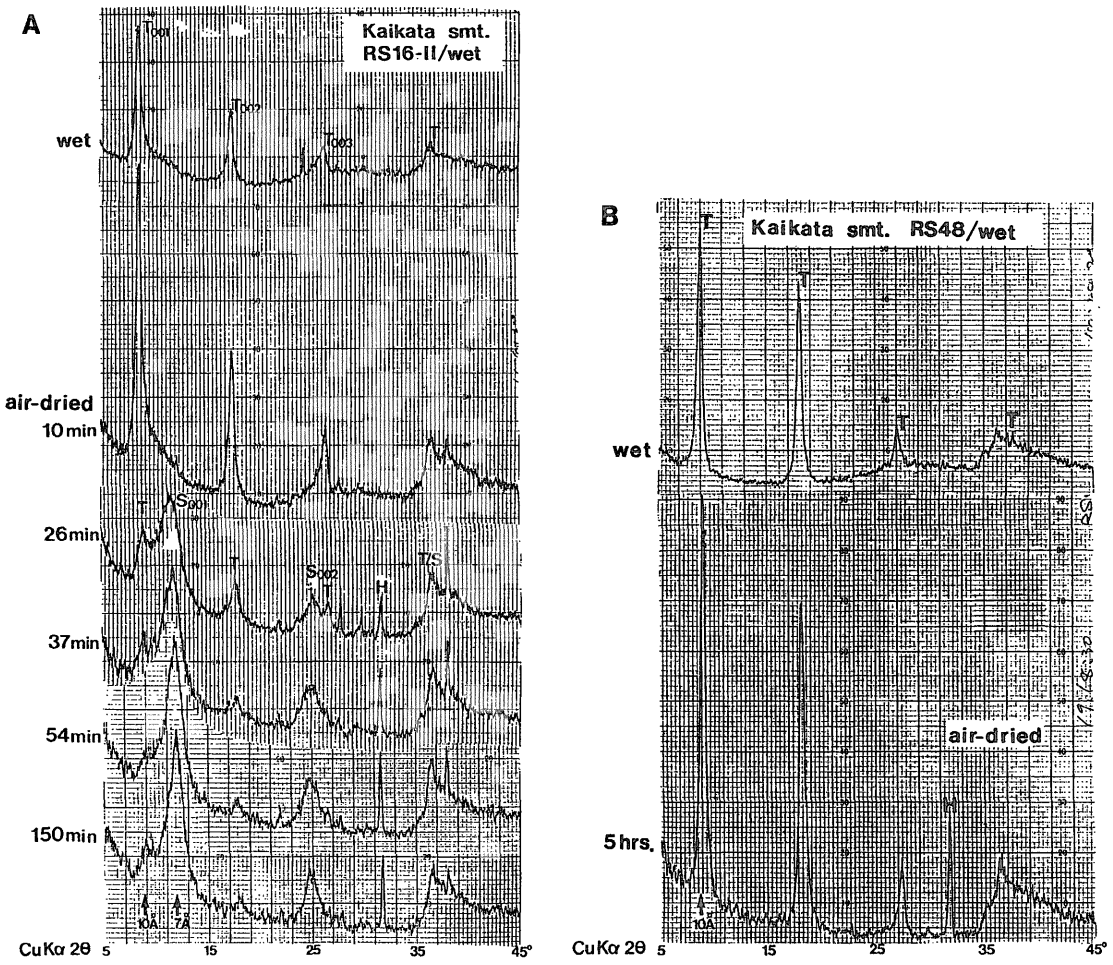

Fig. 5 Typical X-ray powder diffraction patterns of hydrothermal manganese deposits. Sharp and strong reflections are characteristic of the deposits. The change of pattern from 10 Å manganate to 7 Å manganate during dehydration is often observed in air at a room temperature (A), while others not (B). T : 10 Å manganate (todorokite), S : 7 Å manganate (unstable todorokite), H : halite after evaporation of sea water.

Table 2 Diagnostic reflections of marine manganates on X-ray diffraction diagram.

In sea water :		
1)	10 and 5 Å	hydrothermal and diagenetic deposits.
2)	7 and 3.5 Å	none.
2)	2.4 and 1.4 Å	hydrothermal, diagenetic, and hydrogenetic deposits.
After air drying at a room temperature :		
1)	10 and 5 Å	hydrothermal and diagenetic deposits.
2)	7 and 3.5 Å	hydrothermal deposits only.
2)	2.4 and 1.4 Å	hydrothermal, diagenetic, and hydrogenetic deposits.

accommodate double layers of H_2O or OH^- stabilized by transition elements between the sheets (Arrhenius *et al.*, 1981 ; Giovanoli, 1980). Buserite is assumed to have tunnel structure of infinite dimension, (3) *Birnessite* : A natural 7 Å phyllomanganate structurally similar to buserite but with a single water molecule layer between the sheets. (4) An iron-manganese mineral, referred to as *vernadite* or δ-MnO_2, is common in manganese nodules of hydrogenetic origin. It is a disorderd mixed-layer iron and manganese oxide mineral composed of randomly-stacked manganate sheets and iron oxide sheets (Burns, 1976 ; Oatwald, 1984).

The marine manganates with a 10 Å X-ray reflection are here referred to as 10 Å manganate while one with a 7 Å reflection like birnessite referred to as 7 Å manganate, because of unsolved problem whether the marine manganates are structural analogues either to land todorokite, birnessite or synthetic buserite. Most of marine 10 Å manganates of this study are similar in XRD pattern to todorokite if they still have a 10 Å-spacing after drying in air. However, some of them can easily transform to 7 Å manganate in air resulting in identical X-ray diffraction patterns to birnessite (Table 2). These two types of stable and unstable 10 Å manganates and intermediate types are often observed in hydrothermal manganese deposits. Some air-dried marine hydrothermal 10 Å manganates and todorokites on land are not distinguishable in XRD patterns. Both of them do not transform to 7 Å manganate on air drying (Fig. 5 and Table 2). At the same time, heavy metal-depleted diagenetic and hydrothermal 10 Å manganates are not chemically distinguishable despthe the different structural stability of 10 Å spacing.

The contents of transition elements, such as Cu, Co and Ni in marine 10 Å manganates vary considerably. Highest metal contents (more than 3 wt.% of Cu plus Ni) are encountered in deep-sea manganese nodules from the Northeastern and Central Pacific (Halbach and Özkara, 1979 ; Usui 1979). In contrast, very low metal contents (usually in the order of tens to one hundred ppm) are characteristic of hydrothermal manganate deposits around vents at spreading centers in the mid-oceanic ridges and in backarc basins (Moore and Vogt, 1976 ; Hoffert *et al.*, 1978 ; Boulegue *et al.*, 1984 ; Tufar *et al.*, 1986). Cu and Ni-enriched 10 Å manganates have not been discovered from the sea floor in this study.

During dehydration experiments on more than forty wet hydrothermal manganese samples some of 10 Å manganates rapidly transformed to 7 Å manganate at a room temperature on air drying whereas the others remained as 10 Å manganate in air or even on heating at 110℃ (Tables 1, 2, and Fig. 5). The Figure 5 is an example of the change in XRD pattern of an unstable 10 Å manganate from the Kaikata Seamount while air drying at a room temperature.

According to the model by Usui *et al.* (1989), it is assumed that marine 10 Å manganates are categorized into two mineral series ; todorokite of hydrothermal origin and buserite of diagenetic origin. All the manganates in these two series are stable as 10 Å manganate in situ on the sea floor. The former series which is likely to be a product from hydrothermal solution (temperature not specified) has a tunnel structure (3 x n ; n=2-5). The latter series comprises 10 Å phyllomanganate, formed in normal deep-sea environment and has various kinds and contents of 10 Å-stabilizing interlayer cations. Both series are linked with unstable 10 Å phyllomanganate formed at low temperature in either hydrothermal or diagenetic environments. The 7 Å manganate, a transformed product from 10 Å manganate, is observed in both diagenetic and hydrothermal deposits.

The transformation from 10 Å manganate to 7 Å manganate is thus due to low structural stability against dehydration either by insufficient interlayer MnO_6 "walls" as in todorokite or by insufficient occupation by stabilizing interlayer cations as in buserite. An identical phase transformation to 7 Å is characteristic both in low-metal diagenetic and synthetic 10 Å manganate, when exposed to air (Usui *et al.*, 1978 ; Mellin, 1981 ; Paterson *et al.*, 1986).

The iron oxide deposits are collected from several localities in the active submarine volcanoes ; the Fukutoku Seamount of the northern Mariana Arc and the Kaikata Seamount of the Izu-Ogasawara Arc. They usually occur in contact with hydrothermal manganese deposits in a form of dense laminated layer of several mm thick. They are characterized by very low concentration

of metal elements, Mu, Cu, Ni, Co, Pb, Zn etc. The SEM micrographs and XRD analysis show amorphous irregular mass of structureless material, sometimes associated by biogenic structure (e. g., iron bacteria). The deposits may be formed at the latest stage of hydrothermal activity at a low temperature probably catalyzed by microbial activity, because high-temperature hydrothermal activity (higher than about 100℃) would have precipitate crystalline goethite or hematite (Bischoff, 1969).

7. Microstructure

The aggregate of crystals sometimes forms irregular mass, randomly oriented mass, matrix of clastics and sands, and rarely elongated cusps under reflecting microscope. SEM observation reveals that the dense layers in hydrothermal manganate deposits of this study are generally composed of flaky or blade-shaped crystals of pure manganates with boxwork or honeycomb strucure (Plate Ⅱ). The size of each manganate crystal is significantly larger than those of hydrogenetic and diagenetic. The crystal of hydrothermal manganate is as long as several hundred μm, and as thick as several μm.

8. Process and environment of deposition

Several localities were surveyed in the Izu-Ogasawara arc and Kyushu-Palau Ridge on regional and small scales. Some of them are likely to be related to active hydrothermal vents while some are regarded to be already extinct. The Kaikata Seamount and Sumisu Rift appear to yield modern hydrothermal manganese deposits. Apart from these active areas, the fossil hydrothermal deposits are often encountered in Nishi-Shichito Ridge (Fig. 3) and Kyushu-Palau Ridge.

1) *Kaikata seamount hydrothermal manganese belt.*

The Kaikata Seamount consists of three major peaks (KN, KM and KS) and a caldera (KC) with the shallowest water depth of 140 meters at peak KM (Fig. 3). Some hydrothermal sulfide mineralization have been discovered at inner walls of KC, while hydrothermal manganese deposits widely covers a flank of peak KM and part of peak KN (Fig. 3).

The major hydrothermal manganate deposit form a NE-SW extending belt about 2 km wide and 10 km long on the northwestern slope of peak KN (Fig. 6). Usui et al. (1989) reported that structural stability of 10 Å manganates, represented as variation in X-ray intensity ratio at 10 Å and 7 Å d-spacings, shows an apparent lateral zoning within the belt. This comparison shows that the stability gradually decreases from the axial part of the belt towards its margins. The most stable 10 Å manganate (stable as 10 Å even at 110℃ drying) consequently occur near the axis (samples RS 16, RS 18, RS 31, RC 448, RC 449). The zonal distribution implies that the hydrothermal water circulates and precipitates near the axis in the Kaikata Seamount hydrothermal belt.

Variation in mineralogy of hydrothermal manganates is not likely due to chemical composition or aging effect, but may be temperature at formation. Other factors, for instance, physico-chemical condition of solution, pressure, and microbial effects should be taken into consideration.

This hypothesis is supported by a very high thermal gradient within volcanic sand sediments, 1.1℃/m, measured at H 316 (Fig. 6) near the belt by using a wire-line heat-flow probe (T. Yamazaki, GSJ, pers. com.). Significantly higher temperatures of bottom sediments than bottom water were successfully measured just beneath the surface hardpan of hydrothermal manganese deposits at two points along the SHINKAI 2000 track (Table 3). These high thermal gradients imply a substantial heat source inside the volcanic body of the seamount.

The occurrence of the hydrothermal manganese deposits on Kaikata Seamount is typical of flat layers of several centimeters in thickness which is overlain by surface hardpan cemented with similar manganate material (Fig. 6). This occurrence suggests that manganates initially precipitated in the very top of the surface sand layers have prevented succeeding discharge of Mn-bearing hydrothermal solution into bottom waters. Thick dense layers of manganates are subsequently precipitated along the occasional cracks on the sea

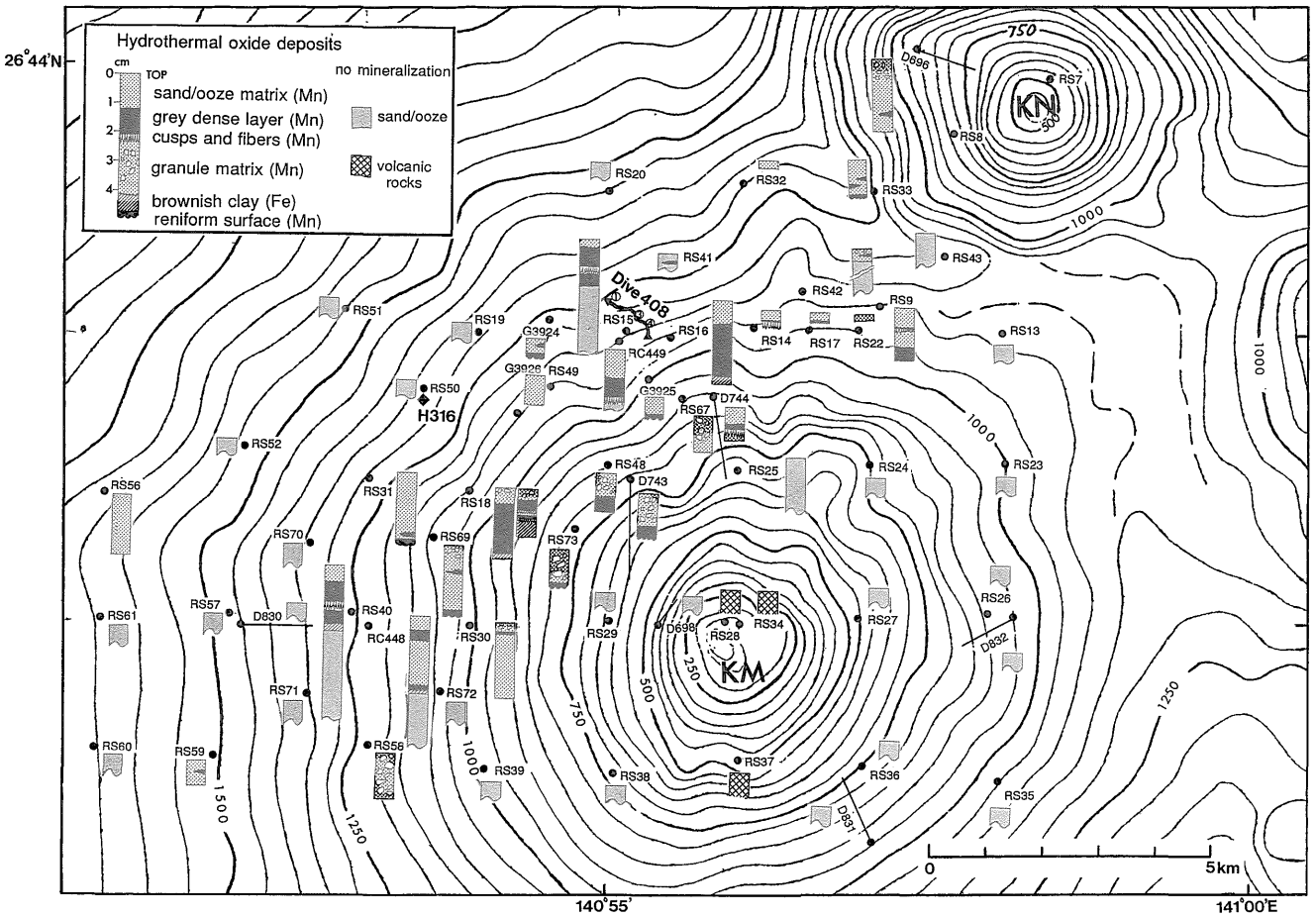

Fig. 6 Distribution of hydrothermal manganese oxide deposits on sea floors of the KM peak, Kaikata Seamount. Lithology of surface several centimeter is shown as columns in the map. Stations of temperature measurement are H316 and st. 1 and st. 3 along the track of submersible observation during Dive 408 with SHINKAI 2000.

Table 3 Temperature of surface sediments in the Kaikata seamount.

Station	H316	Dive 408 st. 1	Dive 408 st. 3
Latitude (N)	26°41.60′	26°42.19′	26°42.13′
Longitude (E)	140°53.51′	140°54.42′	140°55.07′
Water depth	1315 m	1219 m	1160 m
Temperature			
1) bottom water	2.82℃	2.66℃	2.81℃
2) sediment -10 cm depth	2.97℃	2.82℃	3.06℃
(difference)	+0.15 deg.	+0.16 deg.	+0.25 deg.
2) sediment -35 cm depth	3.25℃	—	—
Method	wire-line probe	thermister of SHINKAI 2000	thermister of SHINKAI 2000
Reference	T. Yamazaki	this study	this study

floor. Microscopic observation clearly revealed a downward of the dense manganate layers. It is also supported by the U-Th dating (T. A. Mellin and J. L. Reyss, pers. com.), which indicates the age of the submetallic dense layers just beneath the sea floor to be 4300 years B. P., while the fresh surface of the bottom side to be younger than 3000 years B. P.

The photographs taken from SHINKAI 2000 (Plate Ⅲ) show frequent occurrence of elongated mounds of 30 to 50 cm in height and several to tens meters in length. This ridge-like mounds seem to be formed when the hydrothermal solution was discharged upward through sandy sediments from subbottom fractures or faults. The Figure 7 demonstrates a probable process of deposition of manganese at the Kaikata Seamount.

2) *Sumisu rift*

A recent rifting of the sea floor has been assumed at the Sumisu Rift (Murakami, 1988 ; Brown and Taylor, 1988). Hydrothermal manganese deposits were collected during the submersible observation with ALVIN on the east wall of the rift in the South Sumisu Basin at a depth of 1770m (Smith *et al.*, 1990) and on a small ridge in the Sumisu Rift (Murakami and Yamazaki, 1990). The east wall consist of normal stepped fault blocks descending to the basin floor of about 2200m depth (Murakami, 1988). Although the basement of each scarp is covered with thick sediments of about 100 m thickness, the scarp is overlain with scarce sediments. The homogeneous hydrothermal manganese deposit, collected near the scarp, may have been derived from low-temperature hydrothermal solution discharged along the fault zones. However, the recent activity seems to be ceased because this deposit is encrusted by very thin (up to 1 mm) hydrogenetic ferromanganese oxide film.

3) *Deposits from the back arc and forearc ridges*

As shown in Figure 2, hydrothermal manganese deposits are widely distributed on the older ridges especially on topographic highs. Collected basaltic rocks from the backarc remnant arc, the Nishi-Shichito Ridge, assign the radiochemical age of 2.2 Ma (Yuasa, 1985). At several localities between 27°N to 34°N, hydrothermal manganese deposits have been collected within calcareous sands, as network veinlets in rocks, nuclei of hydrogenetic nodules, and substrate of hydrogenetic ferromanganese crusts.

The flat-topped seamount in the Nishi-Shichito

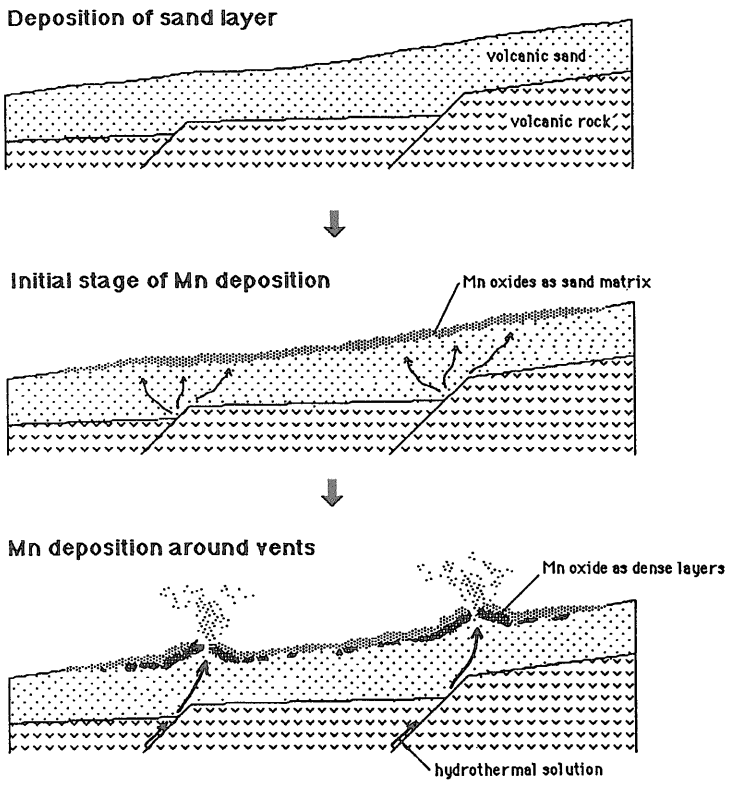

Fig. 7 Schematic diagram showing process of deposition of hydrothermal manganese oxides. The stage of fracturing or faulting of sustrate volcanic rocks is not specified.

Ridge (Tenwa seamount, Usui *et al.*, 1986) is partly covered with several to ten centimeter thick hydrothermal manganese deposits and nontronite claystone. The area of distribution of hydrothermal deposits is as large as several kilometers in length, near the crest of the seamount. The age of the hydrothermal manganate is estimated as 0.4Ma (Mellin and Reyss, pers. com.) Similar occurrence is also common in the forearc ridge, the Shin-Kurose Ridge and the Ogasawara Ridge (Yuasa and Yokota, 1984). Radiochemical dating of rocks from the Shin-Kurose Ridge assigns Paleogene (Honza *et al.*, 1982). One of the age of hydrothermal manganese deposits is older than 0.5Ma (Mellin and Reyss, pers. com.)

4) *Deposits from the Paleogene island arc, the Kyushu-Palau Ridge*

At two seamounts of the ridge, hydrothermal manganese deposits serve as nucleus of hydrogenetic nodules of 6 to 8 cm in diameter (Plate Ⅱ). Surrounding encrustation of hydrogenetic ferromanganese layers are 2 to 3 cm in thickness, and contain 15 to 25 wt.% iron and manganese. The basement andesitic rock implies that the ridge was formed at the ancient island-arc system during Paleogene (Seno and Maruyama, 1984 ; Mrozowski and Hayes, 1979). The occurrence of thick hydrogenetic ferromanganese layer, 10 cm in maximum, is consistent with the estimated age of the ancient island arc. The fragment of hydrothermal manganese oxide deposits inside the nodules is, therefore, a record of ancient hydrothermal activity in the stage of island-arc formation.

9. Summary

The reconnaissance and detailed geological surveys revealed extensive distribution of hydrothermal manganese deposits both in the active volcanic chains and on the remnant inactive ridges. The deposits are most dominant at topographic highs of active submarine volcanoes and backarc rifts, e.g., the Kaikata Seamount and the Sumisu Rift. The detailed mapping and analysis on the deposits from Kaikata Seamount implies upward migration of low-temperature hydrothermal solution through volcanic sands and possible recent precipitation at the sea floor, despite the fact that in-situ temperature measurement shows no evidence of high-temperature hydrothermal vents. The zonal distribution of structural stability of 10 Å manganates suggests decreasing intensity of hydrothermal activity from the axis towards its margins in the hydrothermal manganese belt (2 ×10km). Hydrothermal manganese deposits from the Sumisu Rift may be related to the activity along the normal stepped faults on the rift wall.

Extensive and common occurrence of hydrothermal manganese deposits may indicate adjacent high-temperature sulfide deposits. The manganese mineral can be used as an indicator of high-temperature hydrothermal activity which is believed to be smaller in scale and harder to locate, because the manganese minerals are resistant to dissolution and alteration in normal sea floor environment. The older deposits within hydrogentic nodules and beneath manganese crusts are records of hydrothermal activity encountered around the ancient island-arc systems.

Acknowledgements : The authors acknowledge GSJ scientific staff for their collaboration and discussion, and crew members of R/V Hakurei-Maru for technical help during research cruises. We are most grateful to Dr. M. Ebihara of the Tokyo Metropolitan University, Dr. T. A. Mellin of the Royal Insititute of Technology, Sweden, and Dr. J. L. Reyss of Centre Faibles Radioactivites, CNRS/CEA, France for their discussion and providing unpublished data. We thank the staff of JAMSTEC and crew of SHINKAI 2000 and M/V Natsushima for their help and cooperation.

References

Arrhenius, G. and Tsai, A.G. (1981) Structure, phase transformation and prebiotic catalysis in marine manganate minerals. *SIO Ref. Ser.*, vol. 81, no. 28, p. 1-19.

————, Cheung, K., Crane, S., Fisk, M., Frazer, J., Korkisch, J., Mellin, T., Makao, S., Tsai, A., and Wolf, G. (1979) Counterions in marine manganates. *In : La Genèse des Nodules de Manganèse,* Clloq. Intl. C.N.R.S. Rept., no. 289, p. 333-356.

Bischoff, J.L. (1969) Goethite-hematite stability relations with relevance to sea water and Red Sea brine system. *In* : E.T. Degens and D.A. Ross (eds.) *Hot Brines and Recent Heavy Metal Deposits in the Red Sea,* p. 402-406.

Boulegue, J., Perseil, E.A., Bemat, M., Dupre, B., Stouff, P. and Francheteau, J. (1984) A high-temperature hydrothermal deposit on the East Pacific Rise near 7 °N. *Earth Planet. Sci. Lett.*, vol. 70, p. 249-259.

Brown, G. and Tailor, B. (1988) Sea-floor mapping of the Sumisu Rift, Izu-Ogasawara (Bonin) Arc. *Bull. Geol. Surv. Japan,* vol. 39, p. 23-38.

Burns, R.G. (1976) The uptake of cobalt into ferromanganese nodules, soils, and synthetic manganese (IV) oxides. *Geochim. Cosmochim. Acta,* vol. 40, p. 95-102.

————, and Burns, V.M. (1979) Manganese oxides. *In* : Burns, R.G. (ed.) *Marine Minerals,* Miner. Soc. Amer. Short Course Notes, vol. 6 , p. 1-46.

————, ———— and Stockman, H.W. (1983) A review of the todorokite-buserite problem : implication to the mineralogy of marine manganese nodules. *Amer. Mineral.*, vol. 68, p. 972-980.

Corliss, J.B., Lyle, M., Dymond, J. and Crane, K. (1978) The geochemistry of hydrothermal mounds near the Galapagos rift. *Earth Planet. Sci. Lett.*, vol. 40. p. 1224.

Cronan, D.S., Glasby, G.P., Moorby, S.A., Thomson, J., Knedler, K.E. and McDougall, J.C. (1982) A submarine hydrothermal manganese deposit from the S.W. Pacific Island Arc. *Nature,* vol. 298, p. 456-458.

Franagan, F.J. and Gottfried, D. (1980) USGS Rock Standards, Ⅲ : Manganese nodule

referance samples USGS-Nod-A-I and USGS-Nod-P-1. Geological Survey professional paper 1155. 39p.

Giovanoli, R. (1980) On natural and synthetic manganese nodules. *In* : I.M. Varentsov and Gy. Grasselly (Eds.), *Geology and Geochemistry of Manganese,* Acad Kiado, Budapest, vol. 1, p. 159-202.

Halbach, P. and Özkara, M.(1979) Morphological and geochemical classification of deepsea ferromanganese nodules and its genetical interpretation. *In* : C. Lalou (ed.) *La Genèse des Nodules de Manganèse,* Colloques Intemationaux du C.N.R.S., no. 289, p. 77-89.

Hein, J.R., Fleishman, C.L., Morgenson, L.A., Bloomer, S.H. and Stem, R.J. (1987) Submarine ferromanganese deposits from the Mariana and Volcano volcanic arcs, West Pacific. *U.S. Geol. Surv. Open File Rept.,* no. 87-281, 1-9 p.

Hoffert, M., Perseil, A., Hekinian, R., Choukroune, P., Needham, H.D., Francheteau, J. and Le Pichon, X. (1978) Hydrothermal deposits sampled by diving saucer in Transform Fault "A" near 37°N on the Mid-Atlantic Ridge, FAMOUS Area. *Oceanologica Acta,* vol. 1, no. 1, p. 699-712.

Honza, E. and Tamaki, K. (1985) The Bonin arc. *In* : A.E.Nair *et al.* (eds) *The Ocean Basins and Margins,* Plenum Publ. Co., N.Y., vol. 7 A, p. 459-502.

————, ————, Yuasa, M., Tanahashi, M. and Nishimura, A. (1982) Geological Map of the Northern Ogasawara Arc, 1 : 1000000. Geological Map Series. Geol. Surv. Japan, no. 17.

Karig, D.S. and Moore G.F. (1975) Tectonic complexities in the Bonin arc system. *Tectonophysics,* vol. 27, p. 97-118.

Leg 126 Shipboard scientific party (1989) Arc volcanism and rifting. *Nature,* vol. 342, p. 18-20.

Lonsdale, P., Burns, V.M. and Fisk, M. (1980) Nodules of hydrothermal birnessite in the caldera of a young seamount. *J. Geol.,* vol. 88, p. 611-618.

Mellin, T.A. (1981) Structural chemistry of synthetic manganate and iron compounds : implication for geochemistry of marine ferromanganese deposits, Ph.D. Thesis, Univ. Gothenburg, Gothenburg, 237p. (unpubl.).

Mizuno, A., Shibata, K., Uchiumi, S., Yuasa, M., Okuda, Y., Nohara, M. and Kinoshita, Y. (1977) Granodiorite from the Minami-koho Seamount on the Kyushu-Palau Ridge, and its K-Ar age. *Bull. Geol. Surv. Japan,* vol. 28, p. 507-512.

Moore, W.S. and Vogt, P.R.(1976) Hydrothermal manganese crusts from two sites near the Galapagos spreading axis. *Earth Planet. Sci. Lett.,* vol. 29, p. 349-356.

Mrozowski, C.L. and Hayes, D.E. (1979) The evolution of the Parece Vela Basin, eastern Philippine Sea. *Earth Planet. Sci. Lett.,* vol. 46, p. 49-67.

Murakami, F. (1988) Structural framework of the Sumisu Rift, Izu-Ogasawara Arc. *Bull. Geol. Surv. Japan,* vol. 39, p. 1-21.

———— and Yamazaki, T. (1990) Observation of pillow lava on the inner volcanoes in the Sumisu Rift. *In* : *Tech. Rept. 6 th Symposium on Deep-sea Research using Submersible "SHINKAI 2000" System,* p. 249-260.

Ostwald, J. (1984) Ferruginous vernadite in an Indian Ocean ferromanganese nodule. *Geol. Mag.,* vol. 121, no. 5, p. 483-488.

Paterson, E., Bunch, J.L. and Clark, D.R. (1986) Cation excange in synthetic manganates : I. Alkylammonium exchange in a synthetic phyllomanganate. *Clay Minerals,* vol. 21, p. 949-955.

Seno, T. and Maruyama, S. (1984) Paleogeographic reconstruction and origin of the Philippine Sea. *Tectonphysics,* vol. 102, p. 53-84.

Scott, R.B., Rina, P.A., McGregorm B.A. and Scott, M.R. (1976a) The TAG hydrothermal field. *Nature,* vol. 251, p. 301-302.

Scott, M.R., Scott, R.B., Rona, P.A., Butler, L.W. and Nalwalk, A.J. (1976b) Rapidly accumulating manganese deposit from the median valley of the Mid-Atlantic Ridge. *Geophys. Res. Lett.,* vol. 1, p. 355-358.

Smith, J.R., Taylor, B., Malahoff, A. and Petersen, L. (1990) Submarine volcanism in the Sumisu Rift, Izu-Bonin Arc : submersible and deep-tow camera results. *Earth Planet. Sci. Lett.,* vol. 100, p. 148-160.

Taylor, B., Hussong, D. and Fryer, P. (1984) Rifting of the Bonin Arc. *EOS,* vol. 65, no. 45, p. 1006.

Tamaki, K. (1985) Two modes of back-arc spreading. *Geology,* vol. 13, p. 475-478.

Terashima, S. (1978) Atomic absorption analy-

sis of Mn, Fe, Cu, Ni, Co, Pb, Zn, Si, Al, Ca, Mg, Na, K, Ti, and Sr in manganese nodules. *Bull. Geol. Surv. Japan,* vol. 29, p. 401-411.

Tufar, W., Tufar, E. and Lange, J. (1986) Ore paragenesis of recent hydrothermal deposits at the Cocos-Nazca plate boundary (Galapagos Rift) at 85°51′ and 85°55′W : complex massive mineralization. *Geol. Rundschau,* vol. 75, p. 829-861.

Turner, S. and Buseck, P.R. (1981) Todorokites : A new family of naturally occurring manganese oxides. *Science,* vol. 203, p. 456-458.

Uraba, T. and Kusakabe, M. (1990) Barite silica chimneys from the Sumisu Rift, Izu-Bonin Arc : possible analog to hematitic chert associated with Kroko deposits. *Earth Planet. Sci. Lett.,* vol. 100, p. 283-290.

Usui, A. (1979) Nickel and copper accumulation as essential elements in 10 Å manganite of deep-sea manganese nodules. *Nature,* vol. 279, p. 411-413.

————, Mellin, T.A., Nohara, M. and Yuasa, M. (1989) Structural stability of marine 10 Å manganates from the Ogasawara (Bonin) Arc : implication for low-temperature hydrothermal activity. *Marine Geology,* vol. 86, p. 41-56.

————, Takenouchi, S. and Shoji, T. (1978) Mineralogy of deep sea manganese nodules and synthesis of manganese oxides : implication to genesis and geochemistry. *Mining Geol.,* vol. 28, p. 405-420.

————, Yuasa, M., Yokota, M., Nishimura, A. and Murakami. F. (1986) Submarine hydrothermal manganese deposits from the Ogasawara (Bonin) Arc, off the Japan Islands. *Mar. Geol.,* vol. 73, p. 311-322.

Yamazaki, T. (1988) Heat flow in the Sumisu Rift, Izu-Ogasawara (Bonin) Arc. *Bull. Geol. Surv. Japan,* vol. 39, p. 63-70.

Yuasa, M. (1985) Sofugan Tectonic Line, a new tectonic boundary separating nothern and southern parts of the Ogasawara (Bonin) Arc, Northwest Pacific. *In* : N.Nasu (Ed.) *Formation of Active Ocean Margins,* Terra Publ., Tokyo, p. 438-496.

———— and Yokota, S. (1984) Hydrothermal manganese and ferromanganese concretions from sea floor of the Ogasawara Arc-Trench region, Northwestern Pacific. *In : United* Nations (*E.S.C.A.P./C.C.O.P.*) *Tech. Bull.,* vol. 15, p. 51-64.

伊豆・小笠原・マリアナ弧及び周辺海域に産する熱水起源マンガン酸化物

臼井　朗・西村　昭

要　旨

工業技術院特別研究「海底熱水活動に伴う重金属資源の評価手法に関する研究」(1984-1989) の一環として白嶺丸による海底地質調査を実施した．小笠原弧の火山フロント上の海形海山には20×20kmの精査海域を設け1マイル間隔の採泥，音波探査，熱流量測定，「しんかい2000」による潜航調査などを実施した．採取した試料は化学分析，鉱物分析，年代測定，微細構造観察等を行った．熱水起源マンガン酸化物は特有の化学組成，鉱物学的特徴をもつため，マンガン団塊・クラストを形成する海水起源及び続成起源の鉄・マンガン酸化物と明確に識別できる．

11回にわたる調査航海の結果からは当海域に広く熱水起源マンガン酸化物が分布することが明らかにされた．これらは火山フロントの海底火山及び背弧リフトでは現世の鉱床として沈澱する一方，第三紀の基盤を持つ残留島弧にも過去の熱水活動の記録を残し，海水起源鉄・マンガン酸化物の下位に団塊の核またはクラストの基盤として分布する．

低温の熱水活動は硫化物を伴う高温の熱水噴出とは様式が異なる．海形海山では砂質堆積物の下部から穏やかに浸出した熱水が海底面の直下に数cmの厚さで盤層を形成し，数kmにわたるきわめて広範囲の海底面に沈澱を生じる．この形成過程は島弧の海底にマンガン酸化物をもたらす低温熱水活動のひとつの典型である可能性が高い．

(受付：1991年6月18日；受理：1991年12月17日)

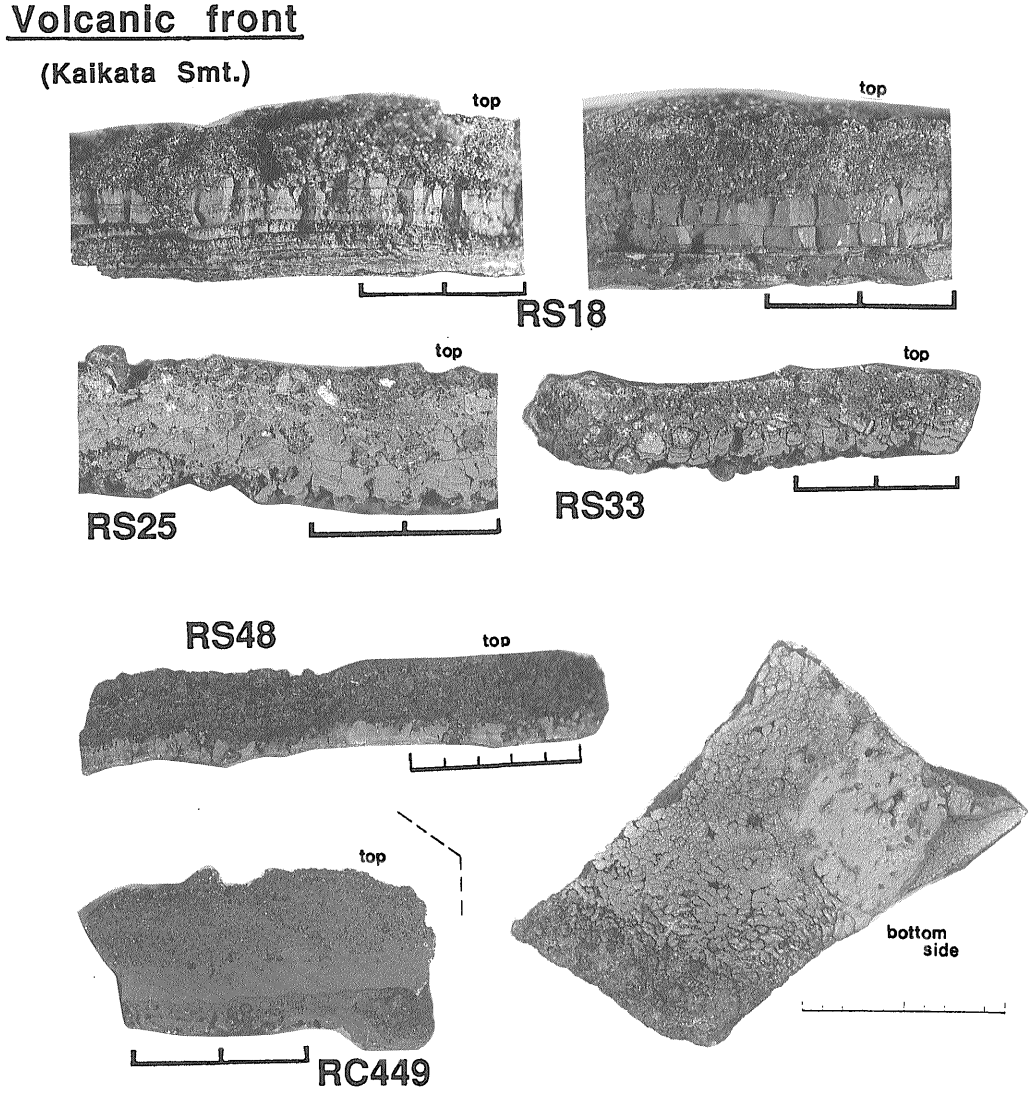

Plate I Typical hydrothermal manganese deposits. Scale in cm.
(A) Kaikata Seamount, volcanic front ; submetallic layers overlain by a sand layer cemented with manganese oxide.

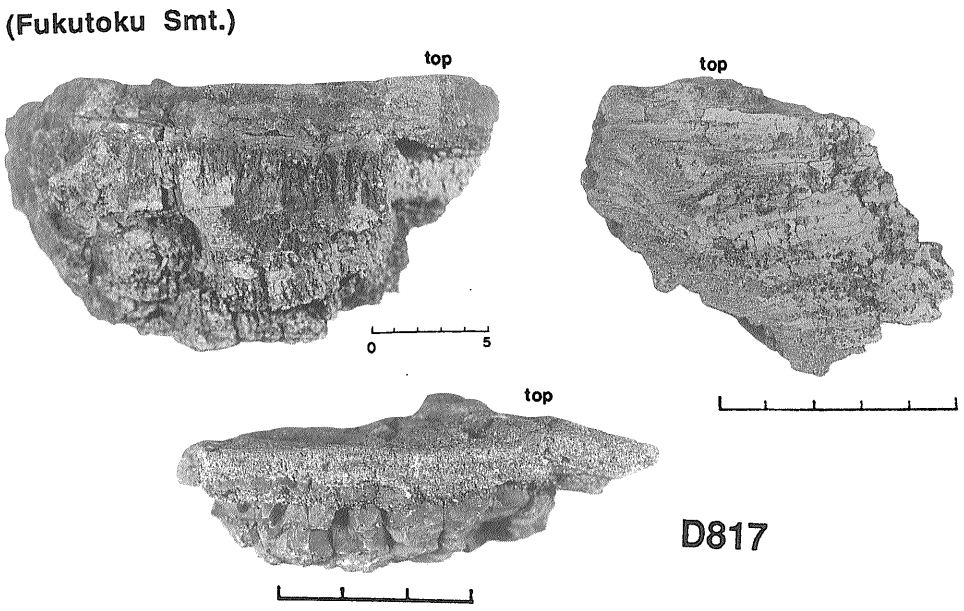

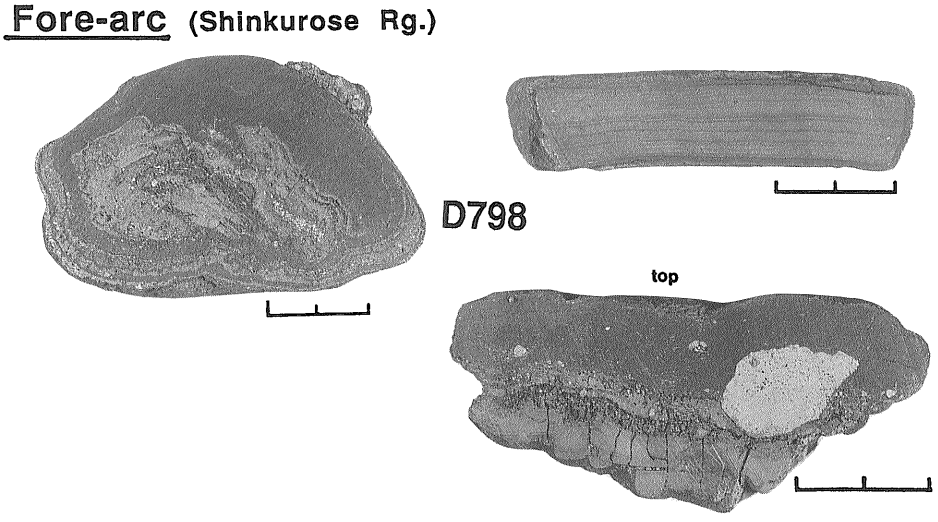

(B/upper) Fukutoku Smt., volcanic front ; large blocks of hydrothermal deposits with downward growth structure from a dredge D817 at 24°03.7′N, 141°40.7′E, water depth 1510 m.
(B/lower) Shin-Kurose Ridge, fore-arc ; hydrothermal oxides are covered with or overlain by younger hydrogenetic ferromanganese oxide layers from a dredge D798 at 30°18.9′N, 140°41.2′E, water depth 1083 m.

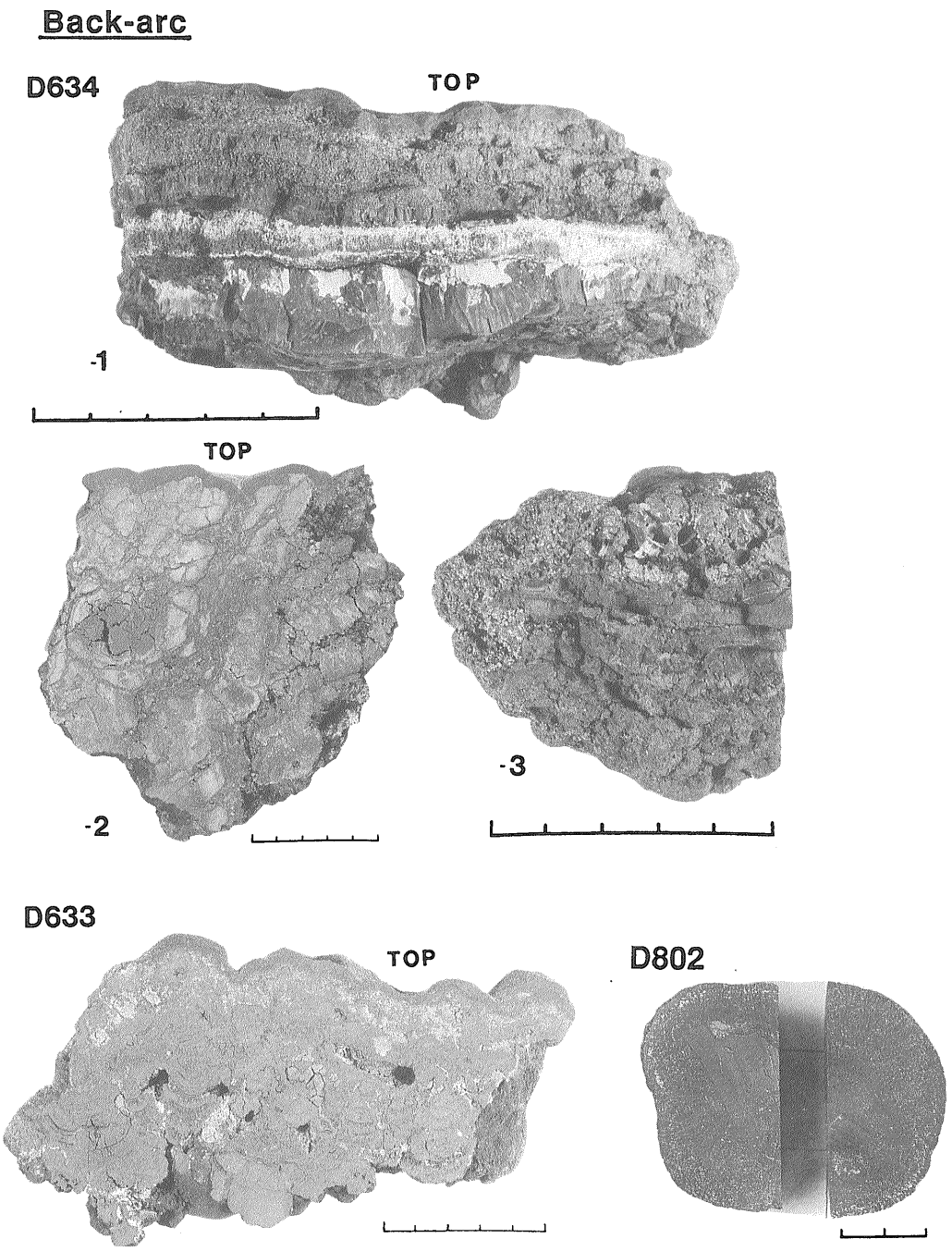

(C) Seamounts in back-arc remnant arc (NSR) ; downward growth structure from dredge sample D634-1 and D633 and network structure within nontronite claystone from sample D634-2 are noted. D634 : 31°22.1′N, 138°46.7′E, water depth 890 m, D633 : 31°30.0′N, 138°21.1′E, water depth 2203 m, D802 : 26°12.0′N, 140°09.2′E, water depth 2515 m.

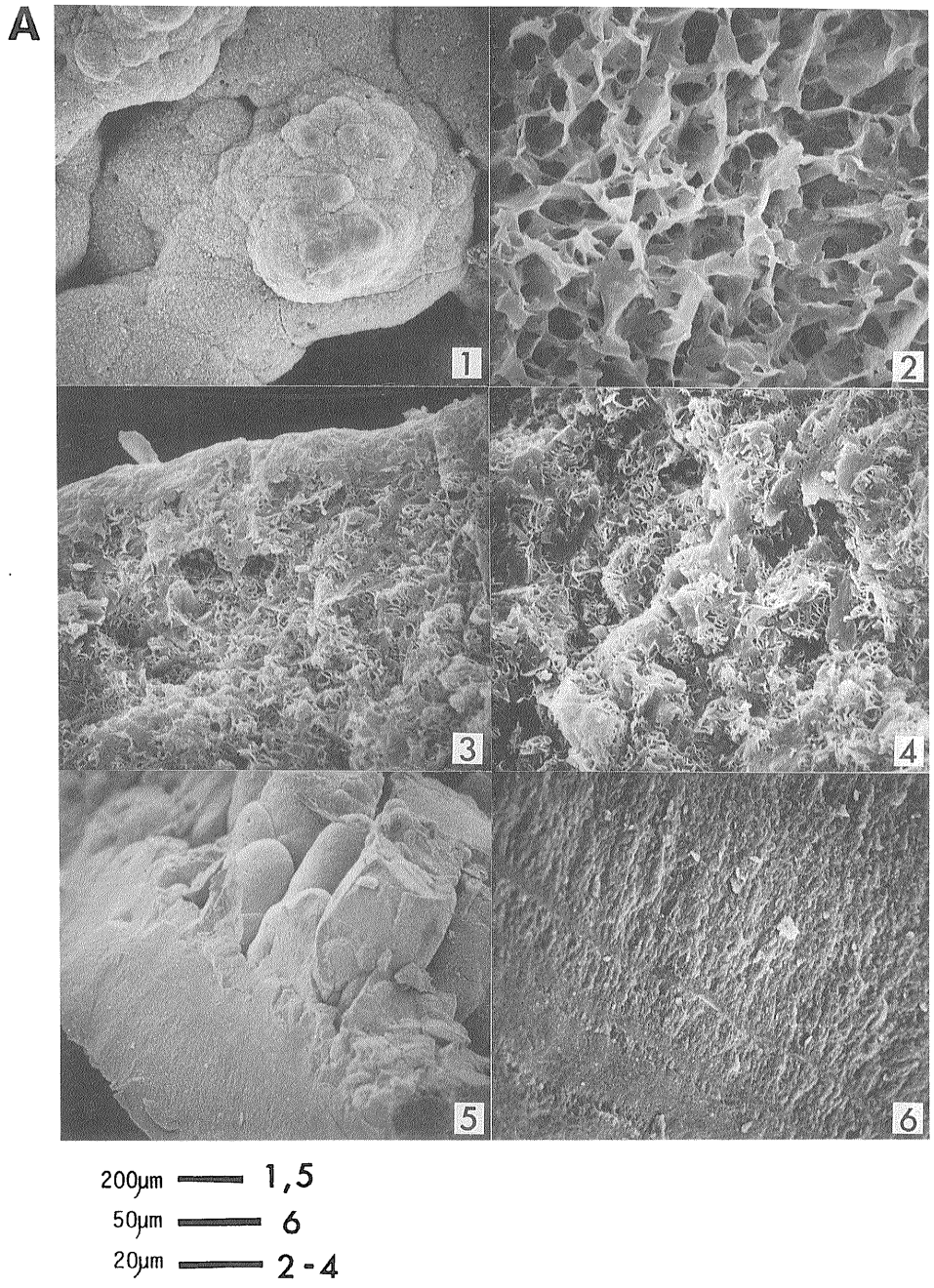

Plate II Scanning electron micrographs of hydrothermal manganese oxides.
A-1) Bottom fresh surface of a dense layer (sample RS 9) ; A-2) close-up of A-1; A-3) broken surface of a dense layer (RS 9) ; A-4) close-up of A-3; A-5) cuspate growth structure (RS 14) ; A-6) close-up of broken surface of A-5.

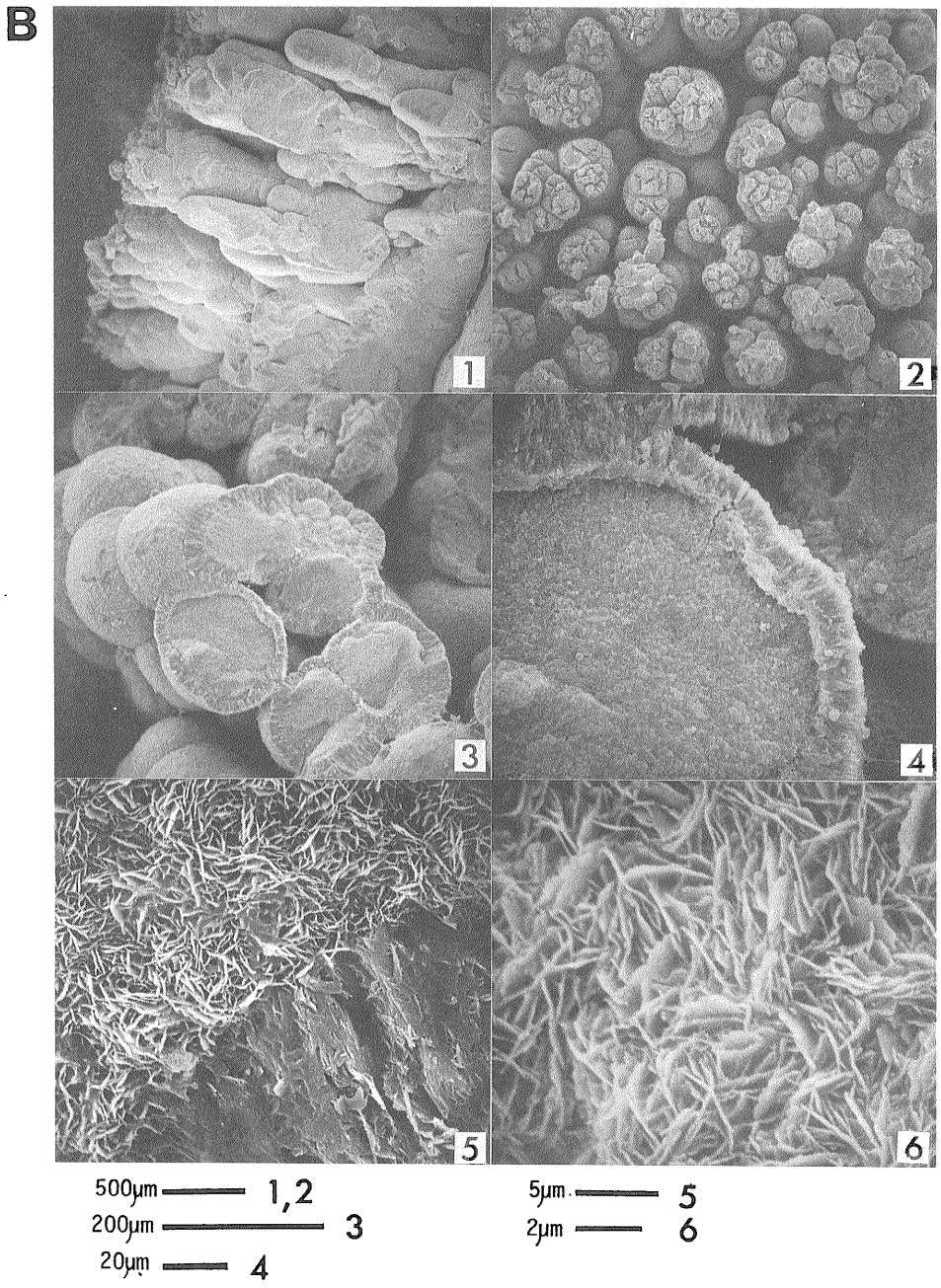

B-1) Side view of growth cusps (RS 14) ; B-2) top view of the cusps (RS 14) ; B-3) broken surface of the cusps ; B-4) and 5) close-up of B3 ; B-6) close-up of B-2.

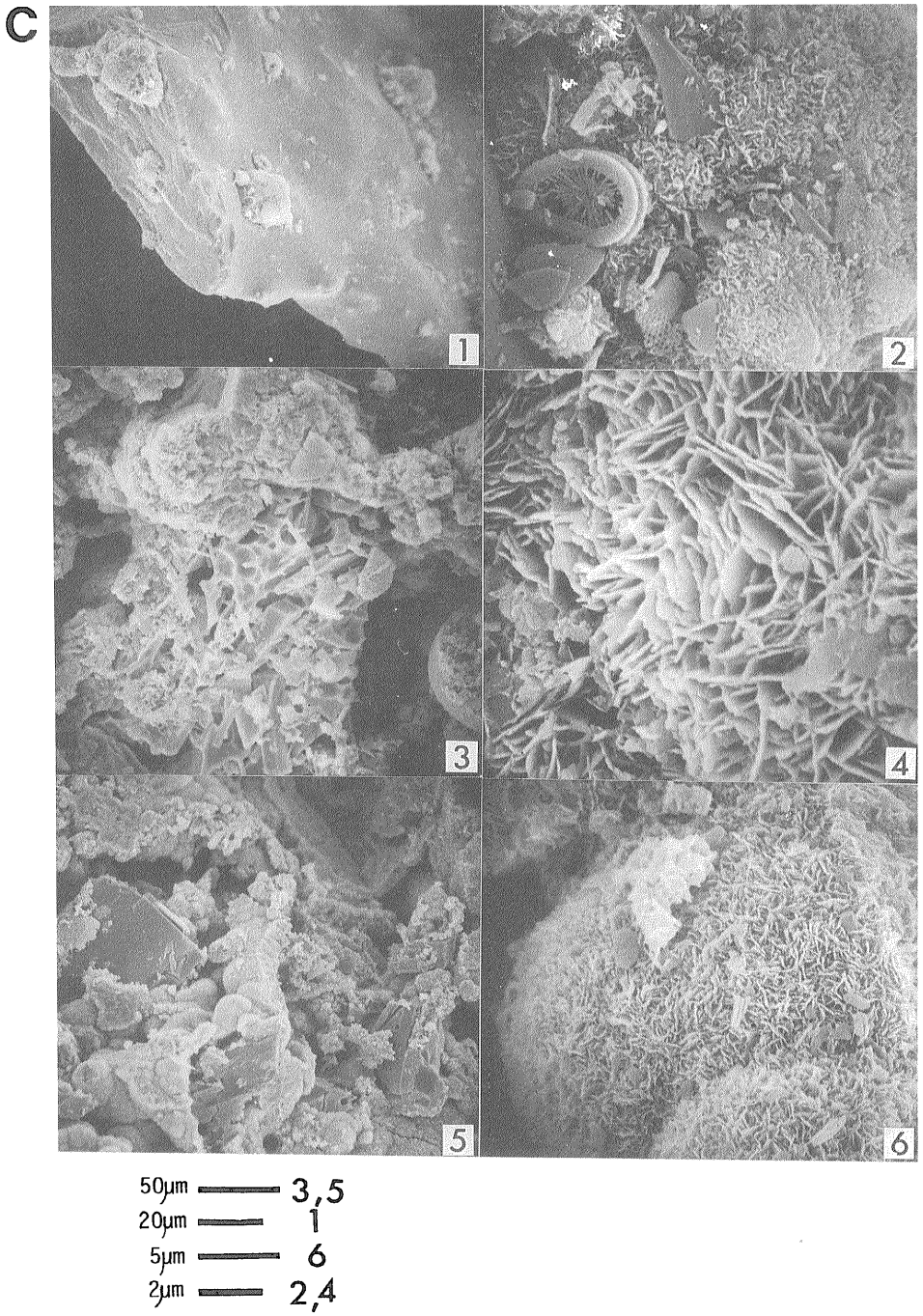

C-1) Volcanic glass grain with manganese oxide stains (RS 15) ; C-2) close-up of C-1 ; C-3) manganese oxide matrix of foram sand (RS 15) ; C-4) close-up of C-3 ; C-5) manganese oxide matrix of foram sand (RS 16) ; C-6) close-up of C-5.

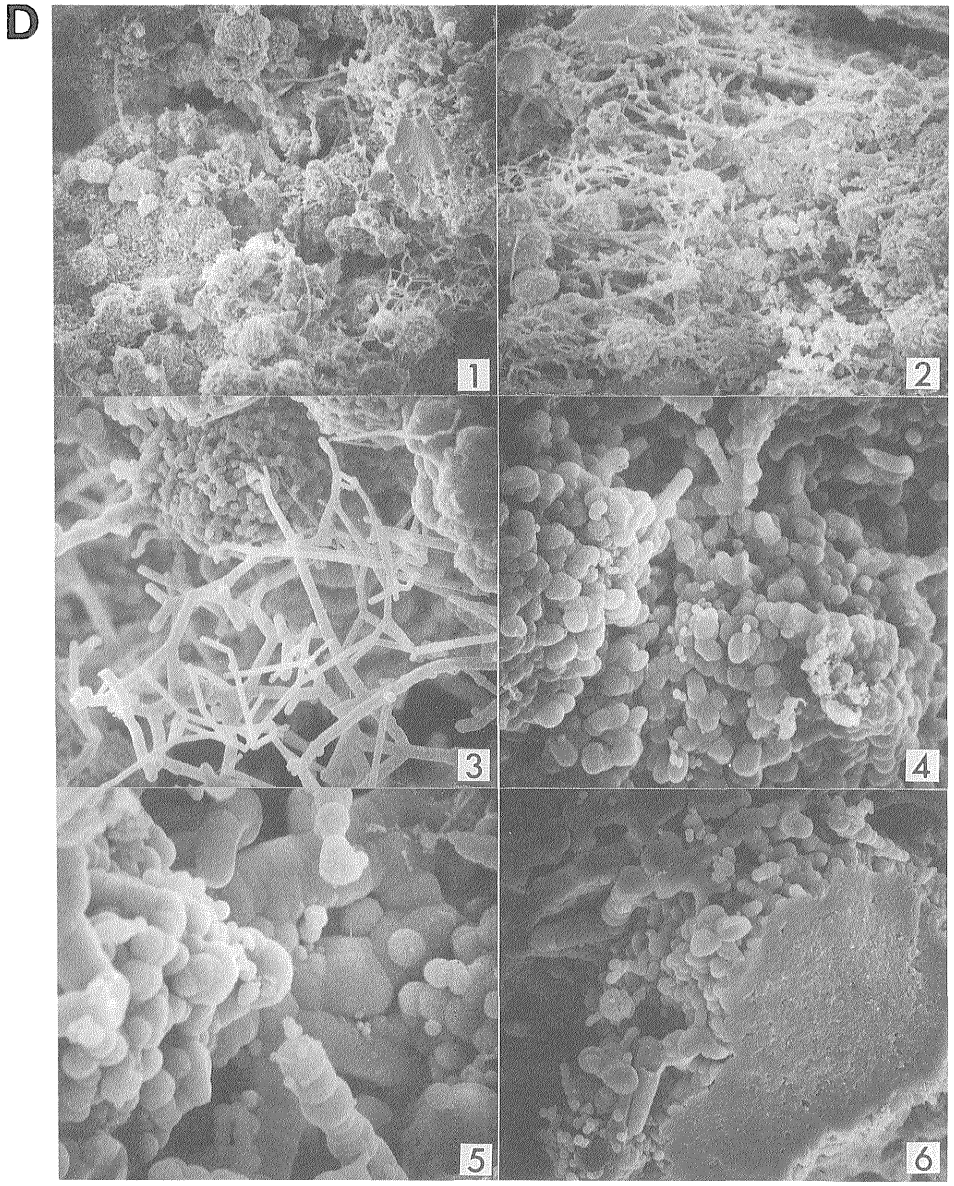

D-1 and D-2) Amorphous iron oxide deposits associated with hydrothermal manganese oxide (RS 16) ; D-3 to D-6) thread and particle like structure formed possibly by microbial process (RS 16).

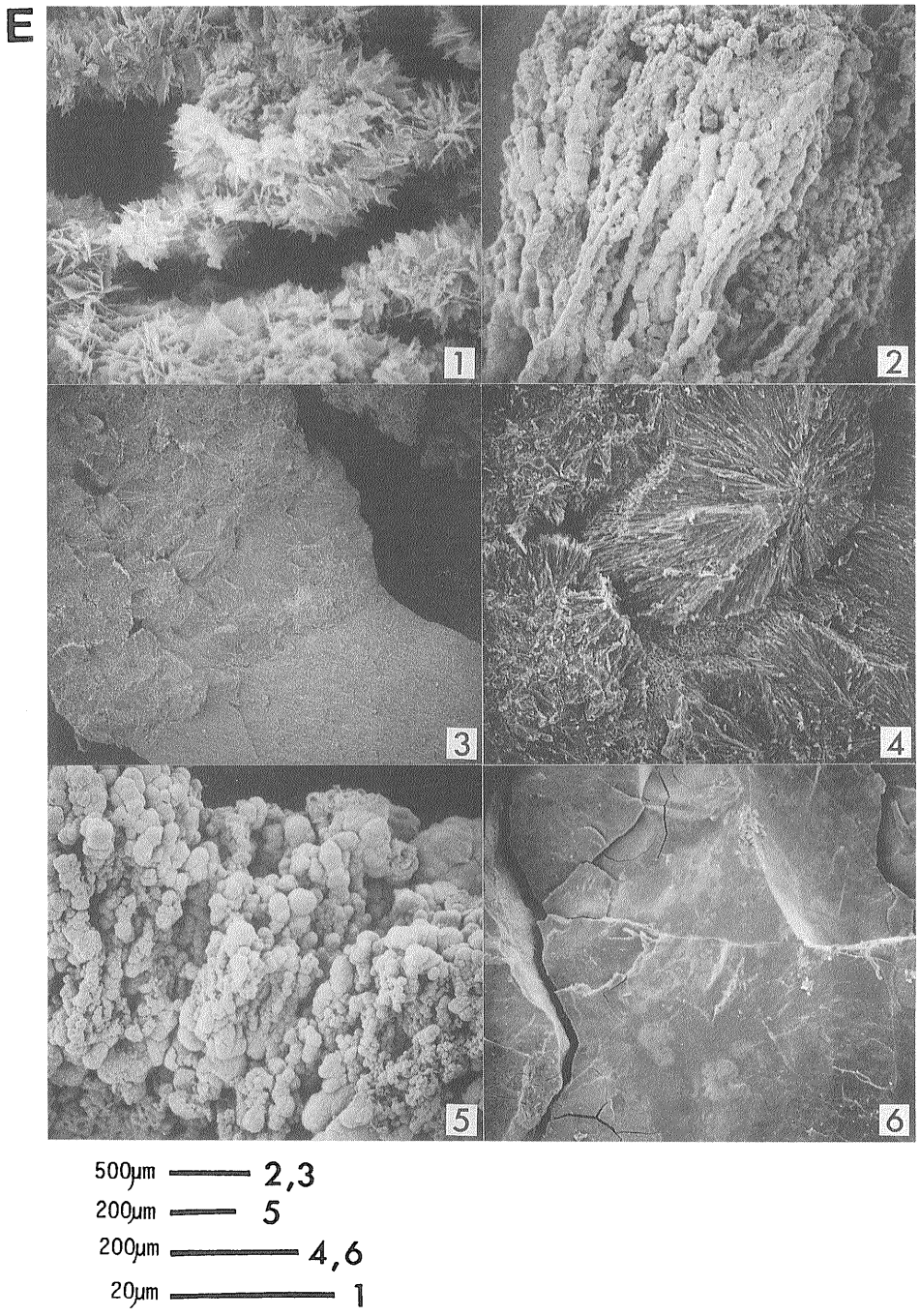

E-1) Blade-like manganate crystals in the vug (D711 ; 24°00.3'N, 141°15.3'E, 840m) ; E-2) thread like form of manganese oxide (D711) ; E-3) dense submetallic aggregate (D711) ; E-4) close-up of E-3 ; E-5) similar to E-2 (D736; 23°37.1'N, 141°48.2'E, 632m) ; E-6) amorphous dense iron oxide deposits (D736).

F

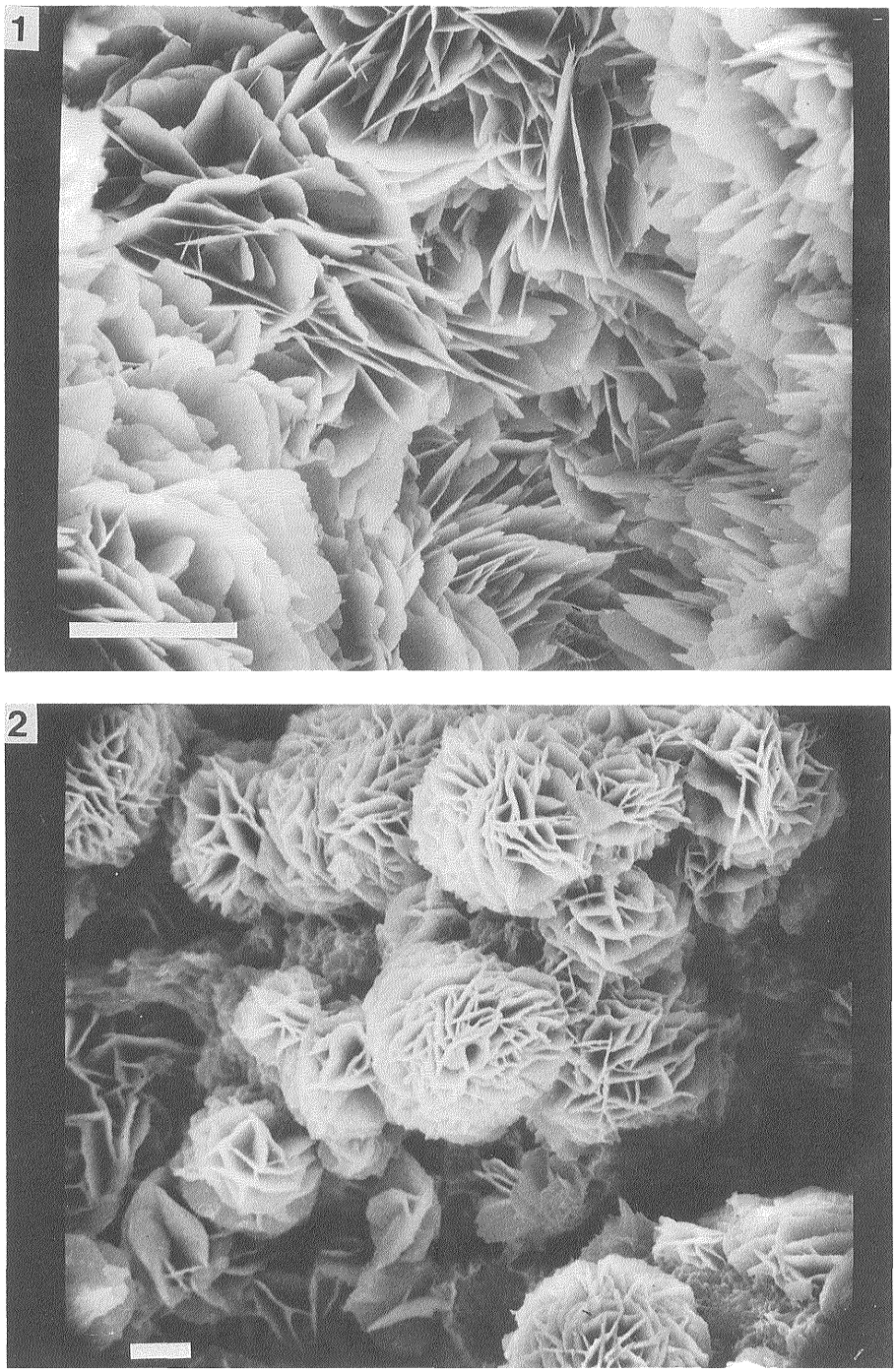

F-1) Blade-like crystals of manganate from submetallic dense layer (D634) ; F-2) surface of veinlets of manganese oxide in a nontronite claystone. Scale bar : 10 μm.

G

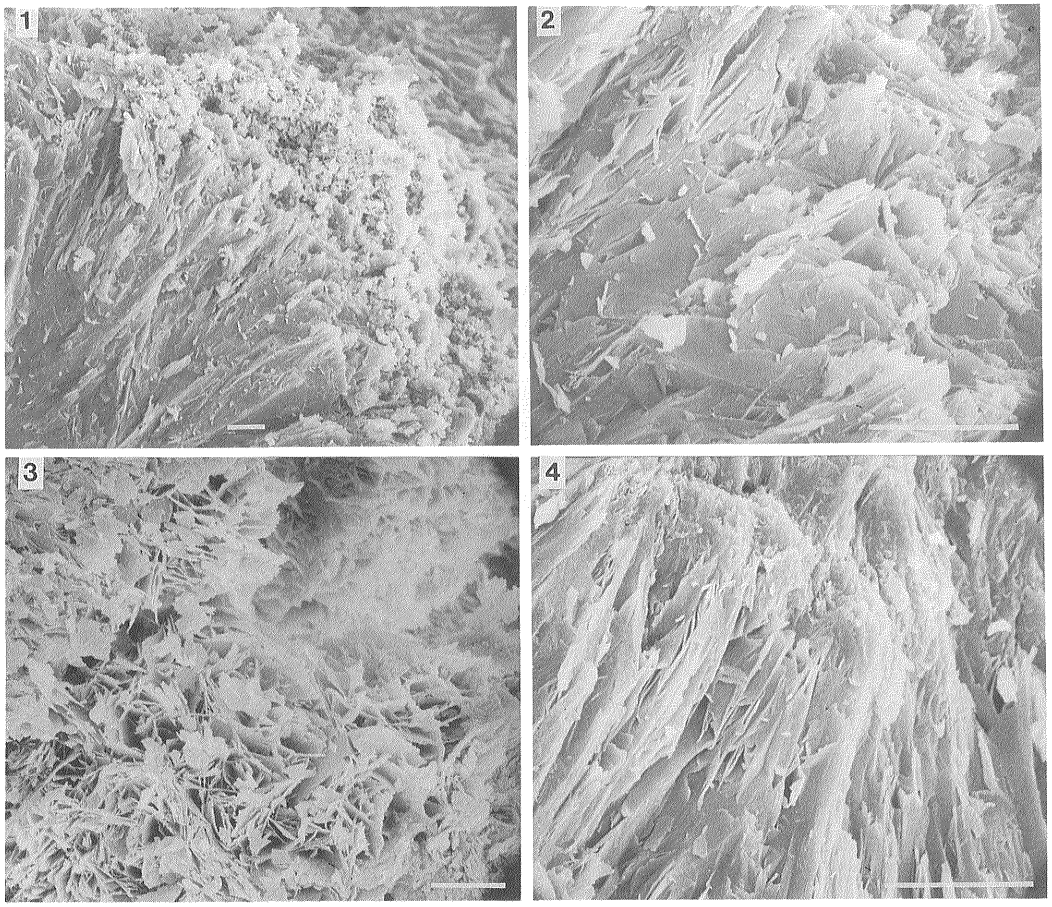

G) Flake or blade-like crystals of manganese oxide in a dense aggregate served as nucleus of manganese nodules from the seamounts of Kyushu-Palau Ridge (D1022 ; D1029). Hatched areas in sketches of nodule section indicate hydrothermal manganese oxide aggregate. Scale bar : 10 μm.

H

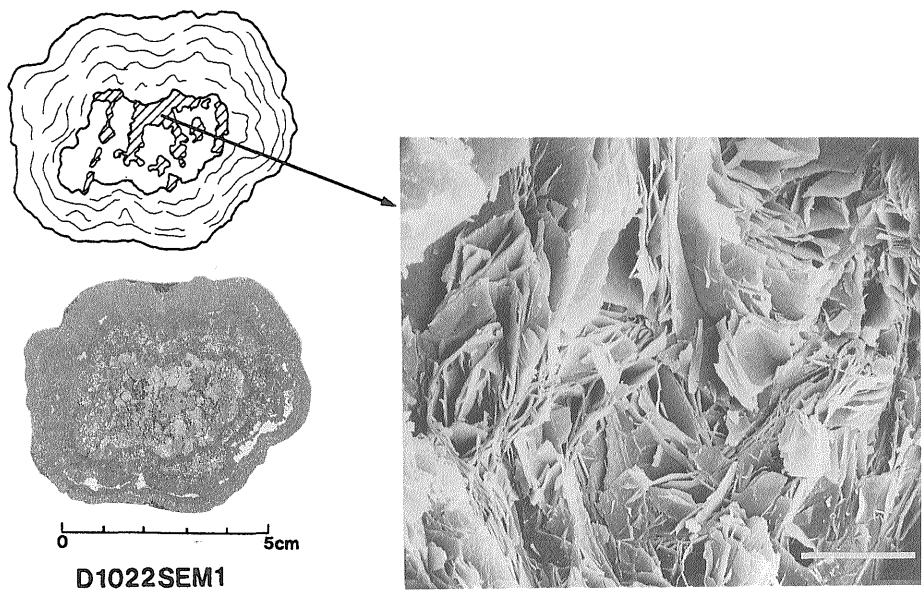

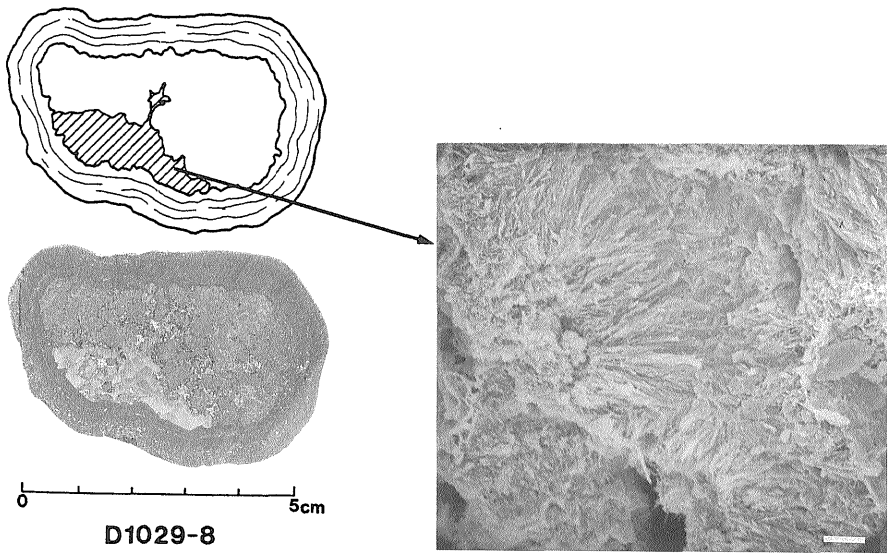

H) Flake or blade-like manganate crystals. Samples are from the same nodules as G). 1-3) D1022, 4) D1029. Scale bar : 10 μm.

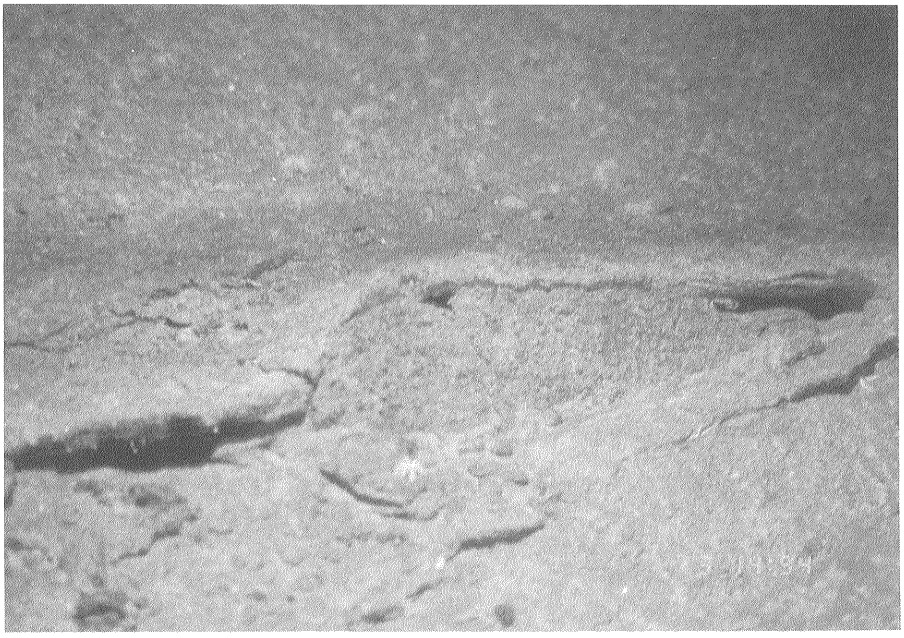

Plate Ⅲ Sea floor photographs taken from SHINKAI 2000. The fractures on the sea floor are usually associated with elongated swells or ridges of 30 to 50 cm in height. Organisms such as Ophiuroids and Crinoids are common around the mounds. Two photographs taken around St. 4 during Dive 408.